UiT
NORGES
ARKTISKE
UNIVERSITET

Faculty of Health Sciences, Institute of Medical Biology (IMB)

The prognostic significance of miR-17-5p and miR-20a-5p in prostate cancer

Lise Martine Ingebriktsen

Master thesis in Biomedicine

August 2018 - May 2019

Supervisors: *Elin Richardsen and co-supervisor Lill-Tove Busund, Translational Cancer Research group, Institute of Medical Biology, UiT The Arctic University of Norway*

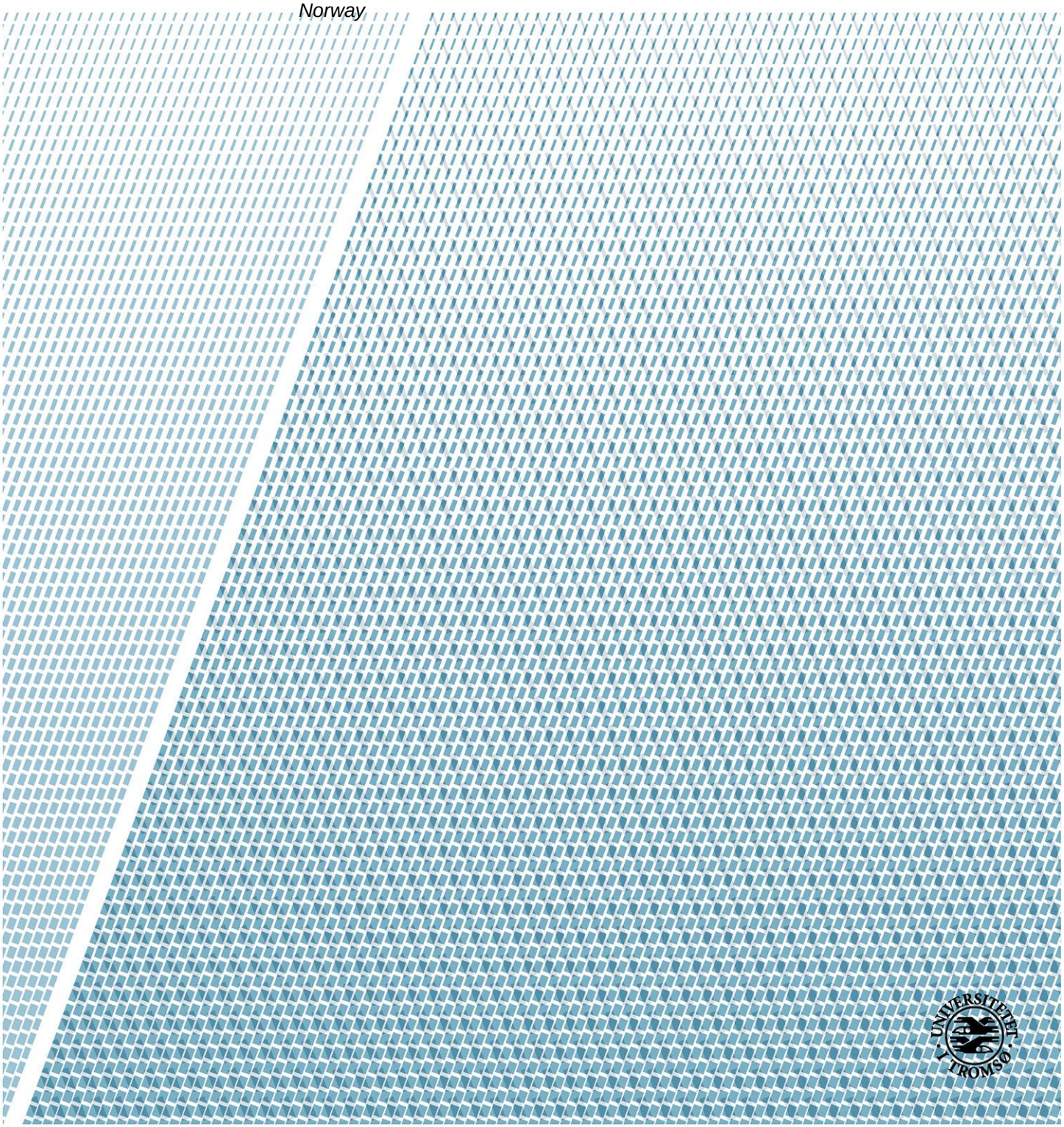

Table of Contents

Acknowledgements

The work of my master thesis was carried out in the period August 2018 - May 2019, at the Translational Cancer Research group, Institute of Medical Biology, University of Tromsø - The Arctic University of Norway.

I feel grateful to have had the opportunity to be a member of this fantastic research group. I want to thank my supervisors Elin Richardsen and Lill-Tove Busund for introducing me to the field of cancer research, and for your consistent support and guidance. I want to especially thank Elin Richardsen. I am truly thankful for your patience and encouragement through this whole process. The valuable skills I have learned from you is priceless. Thank you for sharing your expertise with me. You are one of the reasons why I am always trying my best.

I would also like to take this opportunity to thank Mona Pedersen. Everything I have learned about *in situ* hybridization today is coming from your generous tutoring and your expertise. It has been a privilege to work in the laboratory with you. A big thanks to all members of the Translational Cancer Research group for your help and support during my master thesis.

I owe thanks to my two roommates. Even though we all struggled with our studies, it was always room for laughter and a glass of wine. Thank you for your love and encouragement. I am going to miss all our adventures together here in Tromsø. Lastly, I want to thank my family. Thank you for your endless love and support. You are simply the best.

Abstract

Background: Prostate cancer (PCa) accounts for extensive mortality and is the second most frequent cancer type occurring in men, acknowledged as a severe health problem globally. Our research focus was to examine biomarkers which may influence cancer development in the human prostate. Therefore, we wanted to examine the microRNAs (miRNAs) miR-17-5p and miR-20a-5p, which are members of the miR-17-92 cluster. In addition, we also wanted to correlate these miRNAs with the proliferation marker Ki-67.

Methods: Based on a large PCa cohort (n = 535), we investigated the prognostic role of miR-17-5p and miR-20a-5p in tumour epithelium (TE) and in tumour stroma (TS) of PCa, combined and separately using *in situ* hybridization. IBM SPSS version 25 was utilized to calculate following endpoints in cancer diseases: biochemical failure (BF), clinical failure (CF) and prostate cancer death (PCD) by performing univariate- and multivariate analyses. The miRNAs were correlated to the proliferation marker Ki-67.

Results: In univariate analysis, we found that high expression of miR-17-5p in TE, and miR-20a-5p in both TE and TS were significant associated with biochemical failure-free survival. In multivariate analysis we found that high expression of miR-20a-5p in TE and Ki-67 in TE came out as significant independent prognosticators for BF. Positive significant correlation between miR-17-5p in TE and Ki-67, and positive significant correlation between miR-20a-5p in TE and Ki-67 was found.

Conclusions: High expression of miR-17-5p and miR-20a-5p in PCa provides prognostic information on cancer tumour progression, as they can yield information about the risk of biochemical failure. Their correlation with the proliferation marker Ki-67 are possibly valuable, whereas they potentially can serve as diagnostic biomarkers in PCa.

Abbreviations

AJCC	American Joint Committee on Cancer
AP	Alkaline Phosphatase
ADT	Androgen Deprivation Therapy
BCIP	5-bromo-4-chloro-3’ indolylphosphate
BF	Biochemical failure
BPH	Benign Prostatic Hyperplasia
CF	Clinical Failure
CI	Confidence interval
CRPC	Castration Resistant Prostate Cancer
DIG	Digoxigenin
DGCR8	DiGeorge syndrome chromosomal Region 8
EAU	European Association of Urology
EGFL7	EGF-like domain-containing protein 7
FDA	US Food and Drug Administration
FFPE	Formalin-Fixed Paraffin-Embedded
HPR	Horseradish Peroxidase
HR	Hazard Ratio
ICC	Intraclass Correlation Coefficient
ISH	*In situ* Hybridization
ISUP	International Society of Urological Pathology
LVI	Lymphovascular Infiltration
LNA™	Locked Nucleic Acids
NE	Normal Epithelium
NCCN	National Comprehensive Cancer Network
NLSH	Nordlandssykehuset Bodø
NS	Normal Stroma
NS	Not Significant
NSCLC	Non-small cell lung cancer
NTB	4-nitro-blue tetrazolium
P	p-value
PCa	Prostate Cancer
PCD	Prostate Cancer Death
PNI	Perineural Infiltration
Preop. PSA	Preoperative PSA
PSA	Prostate Specific Antigen
PSM	Positive Surgical Margin
QOL	Quality of Life
qPCR	quantitative Polymerase Chain Reaction
RISC	RNA-Induced Silencing Complex
St. Olav	St. Olavs Hospital/Trondheim Universitetssykehus
Tm	The melting temperature of an oligonucleotide
TMA	Tissue Micro Array
UNN	University Hospital of North Norway
UTR	Untranslated Region
WHO	World Health Organization

1 Introduction

1.1 Epidemiology

1.1.1 Prostate cancer: allegedly *a very rare disease*

The first case of prostate cancer (PCa) was described in 1853 by a surgeon at The London Hospital who reported it as "*a very rare disease*" [1]. Today, 166 years later, PCa is globally acknowledged as a severe health problem [1]. PCa accounts for extensive mortality globally with approximately 1.600 000 new cases each year, and 366.000 deaths annually, which is 58.519 more deaths than registered in 2012 (Figure 1) [2], representing a massive challenge for patients, relatives, and healthcare [3-5]. PCa ranks as number five as leading cause of cancer mortality, furthermore being the second most frequent cancer type occurring in men, and in the United States alone it was estimated 164.690 diagnosed PCa patients in 2018. PCa incidence rates are notably higher in high resource regions of the world, including Australia, the majority of Scandinavia and North America, compared to the poor developed regions of the world, which in contrast suffers from higher mortality rates [4, 6].

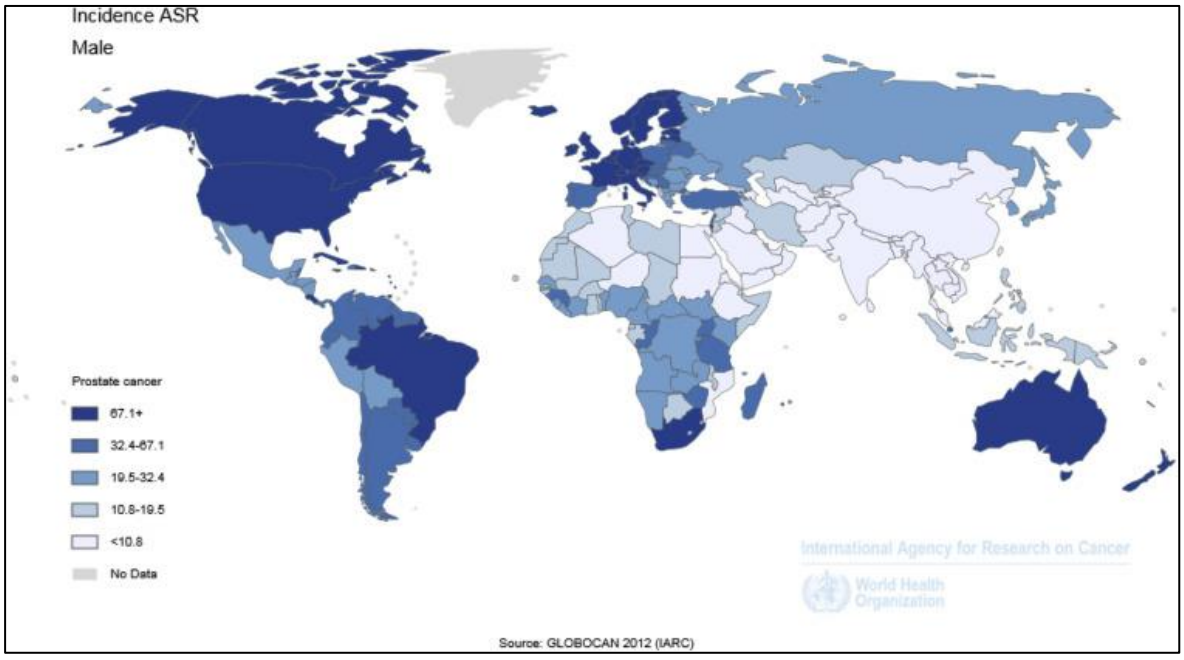

Figure 1: Prostate cancer incidence around the world. Illustration of the geographical distribution of the incidence rate of PCa globally in 2012. High incidence areas are showed in dark blue, which includes Australia, most of Scandinavia, and north America (Awaiting permission: Hassanipour-Azgomi, S, *et al*. 2016) [2].

In Norway, PCa is the most common form of cancer in men. In the recent years, there have been around 5.000 new cases of prostate cancer diagnosed each year. In 2017, a total of 4983 men were diagnosed with PCa [7]. Considerably fewer men dies of PCa every year, and despite an increase in the number of elderly men in the Norwegian population, the number of men dying of PCa have been relatively stable, thus indicating that the mortality rate of PCa have decreased. The number of patients being diagnosed annually with PCa are more than the number of men dying of the disease. As a result, the number of men that are currently living with, and need some sort of follow-up for their disease, have doubled the last ten years [7].

The incidence rate of PCa in various age groups have gradually increased from 1960 to 2017 (Figure 2), and especially increased in the mid-1990s, when the blood test Prostate Specific Antigen (PSA) was introduced in Norway, hence more active diagnostics of the disease may explain this escaladed increase [7].

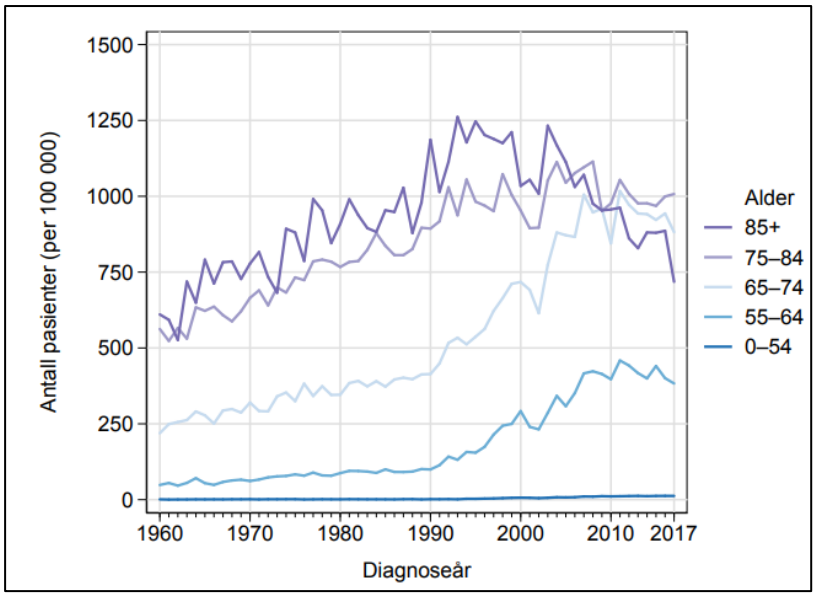

Figure 2: Incidence rate for PCa for various age groups (54-85+) in Norway. Y-axis represents number of patients per 100 000, while x-axis represents diagnose year (1960-2017). The introduction of Prostate Specific Antigen in the 1990s contributed to a significant increase in active PCa diagnosis in Norway (Kreftregisteret, 2018) [7].

1.2 Prostate anatomy

1.2.1 The human prostate gland

The human prostate is a relatively small organ with the size of a walnut, that is located in front of the rectum, at the base of the urinary bladder. This male accessory gland is the site of origin for the two most prevalent diseases occurring in elderly men; Benign prostatic hyperplasia (BPH), and PCa. Thus, this organ demands more attention than what one would normally expect from its relatively small size. It is composed of a base, an apex, posterior, anterior, and inferior lateral surfaces [8]. The upper part of the urethra, commonly known as the tube that transports urine out of the body, is wrapped by the prostate. Moreover, in contrary to what one would intuitively expect, the top of the prostate is called the base and the bottom is called the apex [9, 10]. Roughly, the prostate gets divided into the peripheral, central, and transition zone, shown in Figure 3 [11].

The peripheral zone comprises approximately 70% of the glandular tissue, hence is the larger of the zones. It surrounds the distal urethra and extends from the base to the apex along the posterior surface and represents the zone which are more common for developing prostate carcinomas. Located between the transition and peripheral zones in the base, making up much of the base of the prostate, is the central zone that surrounds the ejaculatory duct, and accounts for approximately 25 % of the glandular tissue. Constituting only around 5 % of the glandular tissue, is the transition zone which surrounds the proximal prostatic urethra. This site is commonly associated with BPH, since the glandular tissue in this portion of the gland enlarges upon BPH development [9-12].

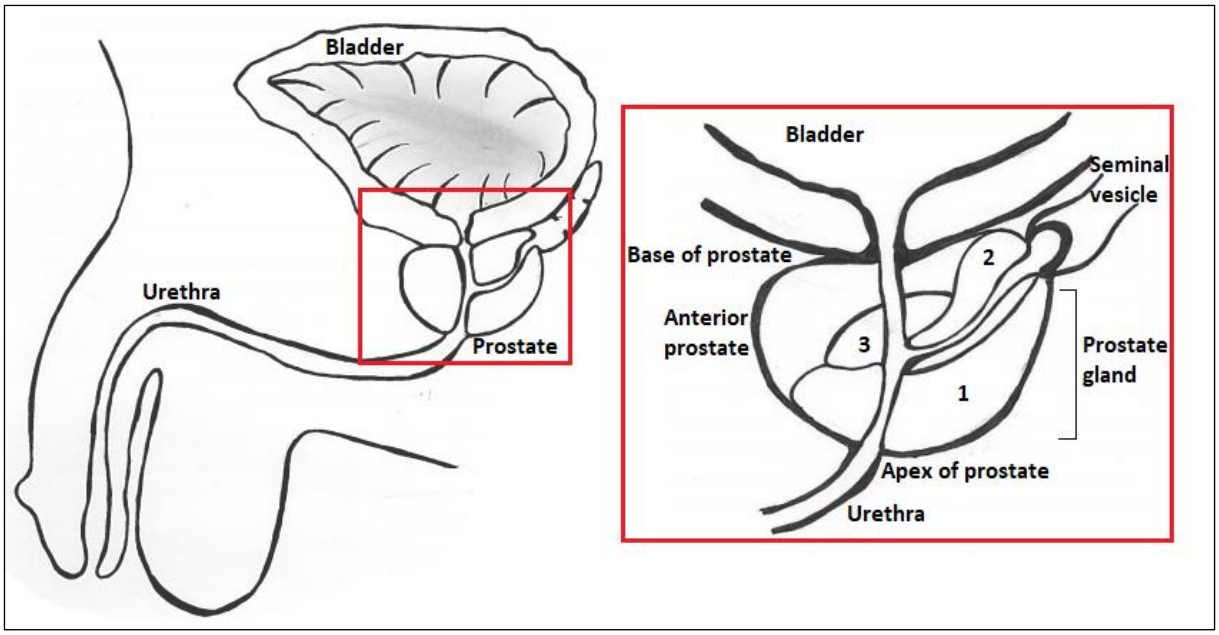

Figure 3: Anatomy of the human prostate gland. The figure presents a simplified illustration of the human prostate gland, and its localisation relative to the urethra and bladder. The prostate gland is divided into the peripheral (1), central (2) and transitional (3) zone. The prostate gland is comprised of a base, an apex, posterior, anterior, and inferior lateral surfaces. PCa development is commonly associated with the peripheral zone, while BPH usually originates in the transition zone. (Lise Martine Ingebriktsen, 2018).

1.3 Diagnosis

1.3.1 Symptoms

Early stage PCa causes few or no symptoms. First when the tumour affects the urine flow, the patient will experience some local symptoms such as a benign enlarged prostate. In cases where the tumour only is located within the prostate, it may cost symptoms like weak or slow urinary stream. These symptoms may also be due to urinary infection, prostatitis (prostate infection), or as mentioned enlarged prostate (BPH). In cases where the tumour has grown beyond the prostate capsule, the patient may experience more painful symptoms, like pain when urinating and blood in the urine. Furthermore, if the disease advances, the patient may experience back and skeletal pain, which is associated with metastatic disease to the bone. Bone metastasis is agonizing for the patient and may lead to neurological symptoms due to the tumour pressing against nerves located in the spine. Some patients with advanced disease may also experience weight loss [13, 14].

1.3.2 Prostate Specific Antigen

PSA is a serine protease which is produced both by normal prostate epithelial cells and PCa cells, and is a member of a family called kallikrein, whereas some of the members are prostate specific. As a protein in semen, PSA is mainly responsible for dissolution of gel in ejaculated seminal fluid. US Food and Drug Administration (FDA) approved PSA as a diagnostic test for early PCa detection in 1994 [15], and since its introduction into clinical practice in 1987, it is still to this day one of the most frequently utilized tests. However, although serum PSA levels can provide helpful information regarding PCa, it has its limitations, and not ideal since it cannot rule out clinically insignificant disease, not being completely disease specific, or lead to early diagnosis. An important feature desired for an optimal diagnostic marker in PCa is to precisely discriminate between malignant and benign prostatic diseases, which PSA fail to achieve. The PSA levels in men is shown to rise with age, and the serum PSA concentration is directly correlated with the prostatic volume and age of the patient. Levels of serum PSA may increase due to damage of normal prostatic anatomy, which is secondary to BPH and PCa. Serum PSA levels may also increase due to excessive amounts of PSA that enters the general circulation, sometimes caused by prostatic trauma. Nevertheless, increased PSA levels is normally the first sign of relapse, and the test is helpful in prediction of possible recurrence of PCa after attempting initial treatment [15-20].

1.4 Staging and classification

1.4.1 Disease progression – from clinically irrelevant to life-threatening

With a range from indolent, localized tumours to aggressive and morbid cancers, PCa represents a biologically and clinically heterogenous disease. Thus, PCa may have a dramatic and aggressive course for some patients, while for others it can progress slowly and even remain untreated without developing clinical symptoms. PCa disease development is known to be closely related to Gleason score, T-stage and PSA, and it is essential that the recommended treatment is based on the patient general condition, such as the patient own expectation for the treatment, life expectancy, and expected benefit of the treatment up against the risk of side effects. Therefore, it is highly important that the patient, in consultation with a doctor, engages in the choice of treatment and evaluate the various

treatment options [7, 21, 22].

The progression of PCa from pre-diagnosis to death can be illustrated as a series of clinical states. These events may be utilized to assess prognosis and different outcomes. The various states can be put together in a progression model presented in Figure 4, that may provide as a framework to assess the different possible outcomes of the disease. The proposed model in Figure 4 can be used to determine where a patient is placed in the clinical spectrum of the disease, and further illustrate the disease as a series of distinct clinical categories, possibly helpful in choosing the appropriate treatment, but also to understand the clinical challenges that are associated with each category [21, 22].

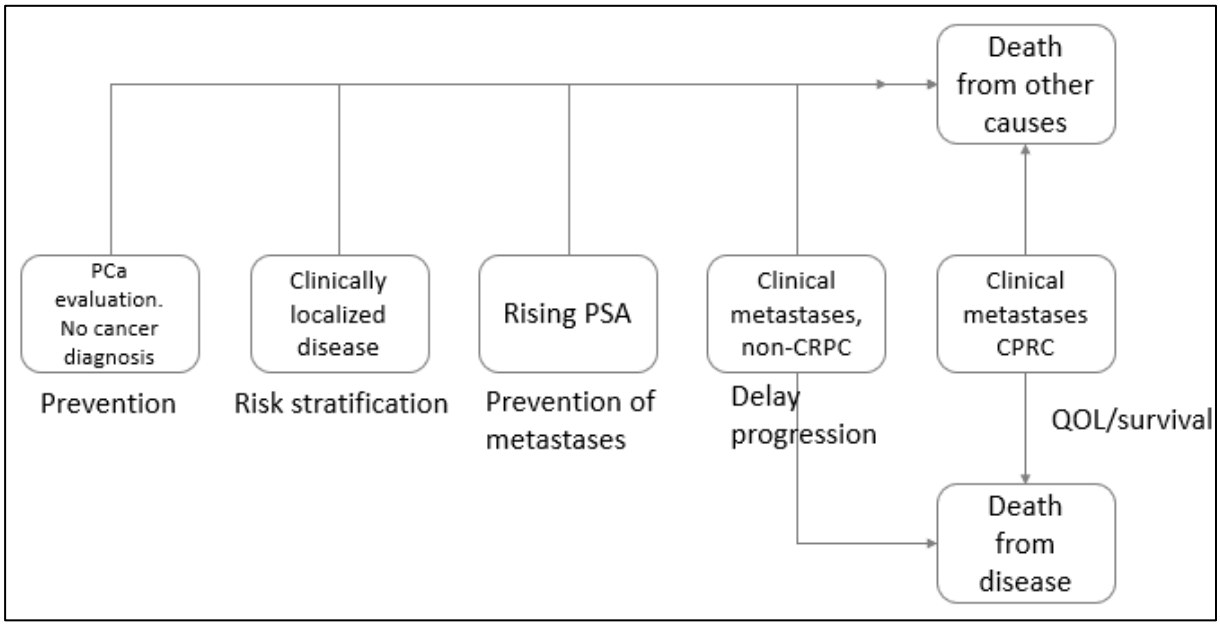

Figure 4: Proposed clinical series model for PCa disease progression. Abbreviations; PCa: Prostate Cancer; PSA: Prostate Specific Antigen; CRPC: Castration-Resistant Prostate Cancer; QOL: Quality Of Life, (Lise Martine Ingebriktsen, 2019).

1.4.2 Gleason grade

The Gleason grading system, first described in 1966 by the pathologist Dr. Donald Gleason, is a grading system utilized to determine the aggressiveness of PCa, furthermore to choose the best suitable treatment option [23, 24]. Until 2000, the Gleason grading system remained mostly unaltered, before it evolved to a significantly modified system after two large consensus meetings (2005 and 2014), conducted by the International Society of Urologic Pathology (ISUP) [23, 25]. The Gleason grading system has been incorporated into the World Health Organization (WHO) classification of prostate cancer, the American Joint Committee on Cancer (AJCC) staging system and the National Comprehensive Cancer Network (NCCN) guidelines as one of the key factors in treatment decision. Moreover, it is favourable that both clinicians and pathologists have sufficient knowledge of the Gleason grading system [25]. Although it has been considerable changes in the histologic and clinical diagnosis of PCa, the Gleason grading system continue as the most robust and strong prognostic predictor in PCa [26].

Figure 5 shows the five histological growth grades determined by the classic Gleason system. Gleason 1 illustrates the best differentiated, and is associated with highly favourable prognosis, in contrast to Gleason 5 illustrating the least differentiated, which is associated with poor prognosis. A primary and secondary grade is given to describe the cells making up the largest and the second largest area of the tumour respectively, based on the architectural growth pattern within the PCa tumours (Figure 5). Higher Gleason scores represents a higher likelihood that the cancer may grow and spread rapidly [24, 25, 27]. The sum of both the primary and secondary patterns yields the Gleason score, and can be exemplified as: Gleason 3 + Gleason 4 = Gleason score 7 (3 + 4 = 7). In cases with only one pattern, both primary and secondary patterns are recognized the same, yielding a Gleason score as such: Gleason 3 + Gleason 3 = Gleason score 6 (3 + 3 = 6) [25, 27].

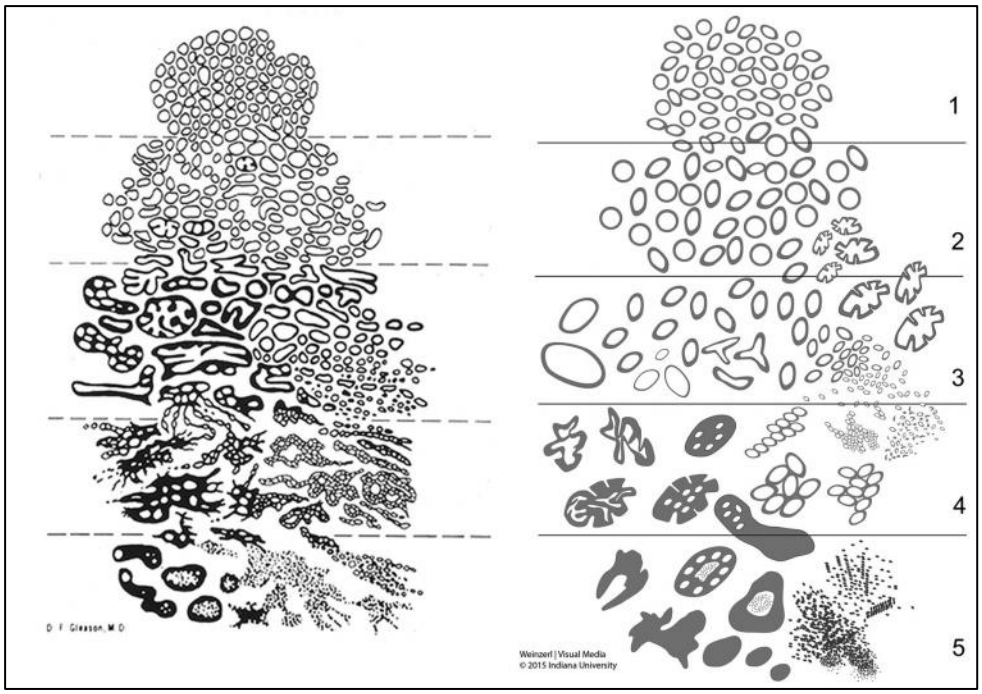

Figure 5: Histologic patterns in PCa. Original (left) and 2015 (right) modified ISUP Gleason schematic diagrams. (Awaiting permission: Epstein J. et al. 2016) [27].

The current application of Gleason grading varies adequately from the original system. Previous scores 2 to 5 are now no longer assigned, and specific patterns defined as a score 6 are currently graded as 7, hence leading to contemporary Gleason score 6 cancers carrying a better prognosis compared to historic score 6 cancers [28].

In 2014, the International Society of Urological Pathologists released supplementary guidance and a revised PCa grading system, called the ISUP Grade Groups. The ISUP Grade Group system is easier, with only five grades, 1 - 5. An important development of the international consensus meeting was the proposal of a new prognostic grade grouping system, which released an improved PCa guiding system, which is called the ISUP Grade Groups. This new system involves that scores less or equal to 6 are collected into ISUP Grade Group 1, Gleason score 3 + 4 = 7 represents ISUP Grade Group 2, Gleason score 4 + 3 = 7 represents ISUP Grade Group 3, Gleason score 4 + 4 = 8 represents ISUP Grade Group 4, and lastly Gleason score 9 to 10 represents ISUP Grade Group 5. ISUP Grade Group 1 is recognized as a low risk group, whereas ISUP Grade Group 4 and 5 is associated with high risk. The current Gleason grading system with the new ISUP grade groups, along with their

respective Gleason scores, histological definitions and risk groups, are presented in Table 1 [25].

Table 1: ISUP Grade Groups, Gleason score, and their respective histological definitions and risk groups.

ISUP Grade Group	Gleason score	Histological definitions	Risk group
1	≤6	Individual, discrete well-formed glands	Low
2	7 (3+4)	Broadly well-formed glands and minor component of poorly-formed/fused/cribriform glands	Intermediate favourable
3	7 (4+3)	Broadly poorly-formed/fused/cribriform glands with minor component of well-formed glands	Intermediate unfavourable
4	8	Merely poorly-formed/fused/cribriform glands OR broadly well-formed glands and minor component lacking glands OR broadly lacking glands and lesser component of well-formed glands	High
5	9 or 10	Lacks gland formation (or with necrosis) with or w/o poorly formed/fused/cribriform glands	High

Retrieved and modified from: (Epstein, J.I. *et al*. The 2014 International Society of Urological Pathology (ISUP) Consensus Conference on Gleason Grading of Prostatic Carcinoma: Definition of Grading Patterns and Proposal for a New Grading System 2016) [27]. Abbreviations; ISUP: International Society of Urologic Pathology.

1.5 Prostate cancer treatment

1.5.1 Treatment guidelines

PCa as a diagnosis can often be overwhelming for the individual patient and close family. PCa is generally a slow growing cancer, and fortunately for the patients, PCa is normally discovered when the tumour is still localized. In Norway, PCa treatment is guided by the Oncology guidelines for prostate cancer published by the European Urologist Association (EAU) [29], and by the national action program for prostate cancer published by the Norwegian Directorate of Health [30].

Today, a wide range of treatment alternatives exists for PCa patients depending on whether the patient suffers from low-, intermediate- or high-risk PCa. Both radiation therapy and prostatectomy are established as curative treatment for PCa, where the former is more frequently offered older men with high-risk PCa, whereas younger men with low-risk cancer more often is treated with prostatectomy. This can be justified by the fact that there is an increased risk of complications after radiation treatment after 20 years, and higher risk for long-term functional disturbances of surgery in elder men compared to younger men [7, 29].

1.5.2 Low- and high-risk prostate cancer

Low-risk PCa is generally defined as a tumour with low risk of progression, PSA level < 10 ng/ml, Gleason Grade score ≤ 6, and is located within the prostate. A large number of men with detected localized PCa will most likely not benefit from definite treatment. Reducing over-treatment in PCa patients have for many years been an ongoing concern, and one of the aims to reduce overtreatment is active surveillance. The purpose of active surveillance is to avoid unnecessary treatment for patients with indolent PCa, and solely treat patients with PCa that shows signs of progression. In case of disease, the surveillance is terminated, and the patient is treated with curative intention [7, 29-32].

High-risk PCa patients are at risk of metastatic progression, and it is commonly defined as PSA ≥ 20, and Gleason Grade score ≥ 8. No consensus is established regarding the optimal treatment for patients with high-risk PCa, however, patients suffering from regionally or

locally localized, high-risk PCa is normally treated with radical prostatectomy or radiation therapy. In addition, surgical castration and androgen deprivation therapy (ADT) are both current treatment options for metastatic PCa. ADT is often recommended to suppress serum testosterone levels in patients with disease progression regardless of previous therapy. Hormone dependent cancers such as PCa may eventually become resistant to treatment (such as surgical castration) after only a couple of years and will continue to progress despite achieving response from hormone treatment such as ADT. The term “castration-resistance” in PCa is often explained by no longer being responsive to castration treatment. Chemotherapy treatment has currently been used in these scenarios, and since the FDA approval in 2004 the chemotherapy agent called Docetaxel (in combination with other medications) have been used as first-line chemotherapy in patients with Castration resistant prostate cancer (CRPC) [31, 33-38].

1.6 Molecular biology of PCa

There are rich chromosomal deviations and genetic mutations found in the genome of PCa patients [39]. Targeted therapy for precise pathways or molecules in advanced PCa has the recent years gained more attention, whereas molecular, genetic, chromosomal, and cellular changes associated with PCa in humans have been investigated [40-42]. Comprehending the molecular biology of PCa is crucial for the improvement of effective therapeutic strategies, especially for aggressive patterns. There are three main types (known today) of chromosomal mutations leading to progression and initiation of PCa; somatic mutations which amplifies oncogenes, somatic mutations resulting in loss-of-function of tumour suppressor genes, and genetic predisposition genes [39, 40, 43]. Chromosomal alterations in prostate tumour cells occur over the course of PCa development [39]. Studies have found both deletions (commonly resulting in loss-of-function of genes), and duplications (commonly resulting in regional gain-of-function of genes) in chromosomal regions [44-46]. This genetic heterogeneity has been an overall challenge not only for PCa treatment, but for cancer treatment in general [39]. Detection and expression of biomarkers are essential for successful identification of PCa. PSA has been a mainstay in therapeutic treatment options and developing diagnostic assays despite the abundance of promising biomarkers. The

continued utilization of PSA demonstrates the challenges of translational research and re-adjust bench to standard clinical use, whereas a potential biomarker must achieve unparalleled benefit in addition to limit overtreatment and overdiagnosis, and to permit clinicians to perform on high-risk localized PCa at limited time. Currently, microRNAs (miRNAs) holds promise and demonstrates potential as biomarkers for PCa [39, 47-49].

1.7 MicroRNA (miRNA)

miRNAs have the last decade emerged as biomarkers for prognosis, cancer diagnosis, therapy, and response prediction in treatment due to ease of detection and their unique specificity. miRNAs are small non-coding molecules, normally consisting of approximately 20 nucleotides. By interacting directly on the 3' untranslated region (UTR) of target messenger RNAs (mRNAs), these single stranded RNAs post transcriptionally controls gene expression by interfering with protein production, which ultimately leads to translational repression or transcript degradation. miRNA expression in the cell can be either temporal (stage of development specific), or spatial (tissue organ specific), furthermore, each miRNA may have several target mRNAs or genes. More than 2500 miRNAs have been identified in the human genome since their discovery in 1993, and it is determined that around 50 % of protein coding genes are being controlled by miRNAs in humans [50, 51]. These fundamental protein coding genes controlled by miRNAs are involved in important biological processes such as programmed cell death, invasion, survival, differentiation, and proliferation. Since critical regulatory functions have been shown by miRNAs in several biological pathways, increased recognition has been provided these non-coding RNAs as interesting candidates as therapeutic tools and as potential diagnostic markers [52-54].

miRNAs act as tumour suppressor miRNAs, or as oncogenic miRNAs (also called oncomiRs), depending on their targets. Tumour suppressor miRNAs suppresses translation of mRNAs that encodes oncoproteins. In contrast, oncogenic miRNAs promote tumorigenesis by blocking translation of mRNAs that encodes tumour suppressor proteins. These miRNA characteristics may result in either blocking or enhancing cancer progression, cancer metastasis, and the probability of cancer resistance to therapy (Figure 6) [53-55].

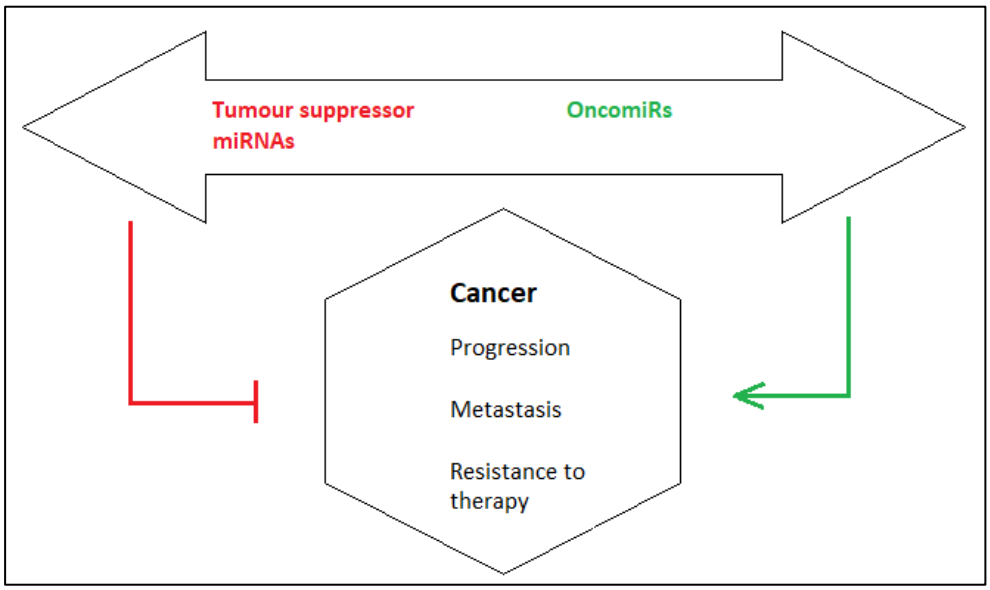

Figure 6: Tumour suppressor miRNAs, or oncogenic miRNAs (oncomiRs). Simplified illustration that presents two roles of miRNAs. Tumour suppressor miRNAs (coloured red), suppresses translation of mRNAs that codes for oncoproteins. OncomiRs (coloured green) promote tumorigenesis by blocking translation of mRNAs coding for tumour suppressor proteins. This results in either blocking or enhancing cancer progression, cancer metastasis, and the probability of cancer resistance to therapy (Lise Martine Ingebriktsen, 2019).

Considering these abilities, there is a broad acceptance that miRNAs possesses an irrefutable role in role in cancer both as suppressors and promoters, including the well-known "Hallmarks of cancer" defined by Hanahan and Weinberg (2000) [56], presented in Figure 7. These hallmarks of cancer were defined as acquired functional capabilities that allows cancer cells to survive, proliferate and distribute. The original six hallmarks of cancer presented by Hanahan and Weinberg includes sustaining proliferative signalling, resistance of cell death, angiogenesis activation, allowing replicative immortality, metastasis and invasion activation, and evasion of growth suppressors [56].

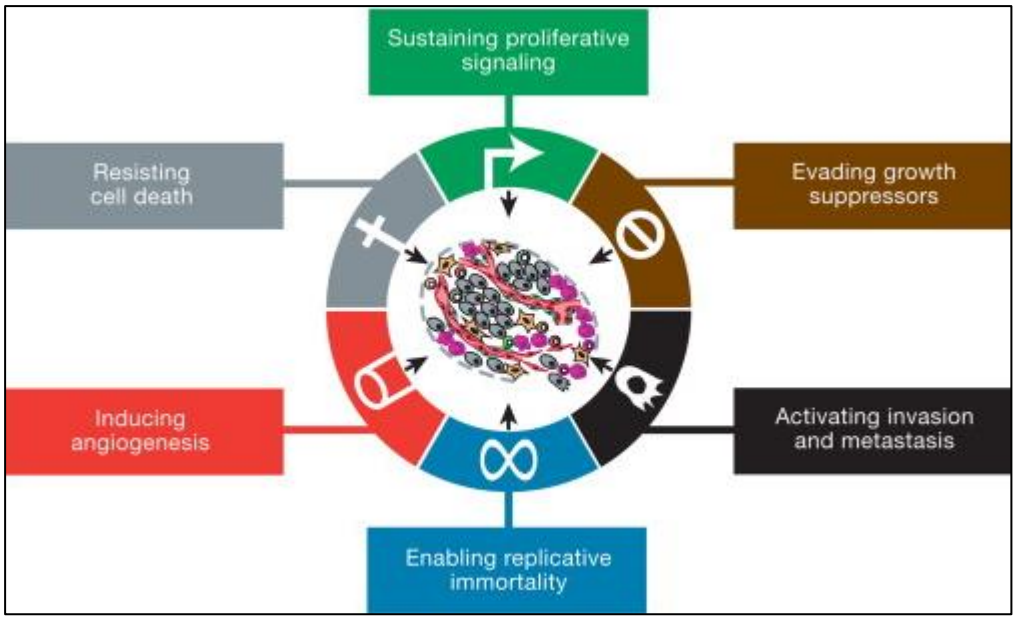

Figure 7: Hallmarks of Cancer. The figure illustrates the six hallmarks of cancer presented by Hanahan and Weinberg in 2000. (Awaiting permission: Hanahan D, Weinberg RA, 2000) [56].

Angiogenesis, known as the growth of new blood vessels from existing vasculature, is a crucial feature for cancer cells to access oxygen and nutrients which are important for proliferation and metastatic spread. miR-93 [57, 58] and miR-296 [59] are both reported to promote angiogenesis and is associated with metastasis activation. The latter is one of the most thoroughly studied miRNA known to promote angiogenesis [60-62]. Additionally, miR-296 is shown to be upregulated in prostate cancer [47]. Another essential cancer hallmark is enabling replicative immortality. miRNA-512-3p is reported to be upregulated in PCa and have a role in promoting proliferation and cell cycle progression in PCa cells [63]. Moreover, several miRNAs have been reported to sustain proliferation and promote cell cycle progression in PCa cells [64-68].

1.7.1 miRNAs as biomarkers

Currently, there is a lack of an optimal early detection method in several types of cancers, including PCa. In the last decades, miRNAs have been broadly investigated in the search of potential biomarkers, which are simply explained as measurable indicators of some biological condition or state. With favourable characteristics such as high chemical stability in both fresh and formalin-fixed tissues, miRNAs have a higher potential as diagnostic

biomarkers compared to longer messenger RNAs or long noncoding RNAs. Since miRNAs are stable, they can be detected in blood, urine, plasma, and other body fluids (liquid biopsies), and have been detected as circulating molecules in these body fluids, and thus suitable for testing in patient samples [52, 54, 69].

Many of the ideal characteristics desired in an ideal biomarker is found in miRNAs. They control a network of targets, a reliable disease indication prior to clinical symptoms, sensitive to pathological or physiological changes, and specific to the desired pathology of interest. miRNA pattern expression may be utilized in classification of sub-populations of patients in the process of choosing the most suitable strategy in clinical practice. It is highly important to discriminate between non-tumour and tumour tissues, and in clinical practice understanding cancer progression and aggressiveness via patient prognosis is crucial [70].

Because of these characteristics, miRNAs have emerged as biomarkers for cancer prognosis, diagnosis, cancer therapy, and prediction of treatment response. Studies investigating potential biomarkers for PCa have greatly expanded, whereas several miRNAs have been suggested as promising candidates. In this study, the prognostic significance of miR-17-5p and miR-20a-5p in PCa tissue were investigated. In 2016, a miRNA microarray analysis was performed by Exiqon (Vedbaek, Denmark), who uses Locked Nucleic Acid-based tools for RNA research (LNA™) which is a technology providing a powerful high-throughput capable of monitoring the expression of thousands of noncoding RNAs simultaneously, whereas miR-17-5p and miR-20a-5p was included. Due to interesting discoveries, including satisfactory staining in breast- and lung cancer tissues, and the fact that both PCa and breast cancer are hormone sensitive cancers, these two miRNAs were of highly interest to investigate PCa specimens as well.

This thesis is part of a larger screening study in our research group, whereas miRNA expression from several selected miRNAs of interest have been studied in both breast cancer tissue, non-small cell lung cancer (NSCLC) tissue, and PCa tissue with the aim to uncover potential prognostic and diagnostic molecular markers. The following miRNAs have

previously been investigated in our research group: miR-141 was studied in PCa tissue, associated with increased risk of biochemical PCa recurrence [71]; miR-205 in PCa, where high expression in normal epithelium was associated with biochemical failure [72]; miR-21 in PCa, detecting high expression of miR-21 in stroma, associated with poor biochemical recurrence-free survival [73]; miR-210 in PCa, reporting overexpression of miR-210 in fibroblasts, independently associated with poor clinical failure free survival [64]; miR-210 in NSCLC, reporting potential independent prognostic impact [74]; miR-155 in NSCLC, reporting positive prognostic impact on survival in both univariate and multivariate analysis [75]; miR-143 and miR-145 in NSCLC, showing high stromal expression of these two miRNAs as gender specific positive prognosticators in early state NSCLC, in addition, assessing tumour suppressor roles of miR-143 and miR-145 in lung cancer [76].

These studies represent a diverse representation of miRNAs that possesses distinct properties and plays unique roles in the aspect of cancer, representing both tumour suppressors and tumour enhancers. Collectively, these previous studies, in addition to the satisfactory staining in breast- and lung cancer tissues of miR-17-5p and miR-20a-5p as mentioned above, and also interesting reports of the miR-17-92 cluster with focus on the roles of miR-17-5p and miR-20a-5p in the literature, we wanted to investigate these miRNAs in PCa.

1.7.2 Biogenesis

In humans, miRNAs are produced by two RNase proteins called Drosha and Dicer. A general overview of the steps involved in the biogenesis is illustrated in Figure 8 [77, 78]. miRNA biogenesis begins in the cell nucleus, where miRNA genes are initially transcribed by RNA polymerase II, yielding long primary transcripts, often referred to as pri-miRNAs (>100 nucleotides) with a 5' guanosine cap and a 3' polyadenylated tail. The pri-miRNA is following processed by a RNase III-type enzyme called Drosha, together with DiGeorge syndrome critical region gene 8 or DGCR8, converting the pri-miRNA into pre-miRNAs, which consists of around 70 nucleotides. These newly transcribed hairpin precursors with their characteristic 5' phosphate and 2-nucleotide 3' overhang is furthermore exported from the

nucleus to the cytoplasm by nuclear transport receptor protein called Exportin 5 [77, 79-81].

When the pre-miRNAs reach the cytoplasm, an enzyme called DICER processes the pre-miRNAs into mature duplexes, around 20 nucleotides long. The two strands are subsequently separated, and one of the strand acts as the guide strand, usually more unstable base pairing at the 5' end, whereas the strand with more stable base pairing at the 5' end, often referred to as the passenger strand, normally gets degraded. The former mentioned strand, the less stable one of the duplexes is incorporated into a multiple-protein nuclease complex, called the RNA induced silencing complex RISC, which is known for regulating protein expression [77, 79-81].

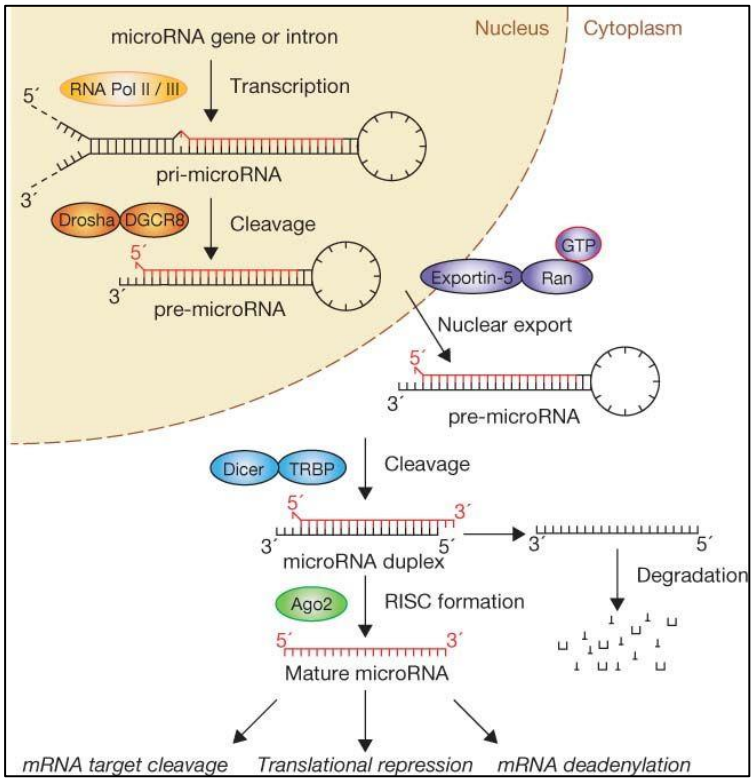

Figure 8: Biogenesis of miRNAs. The miRNA gene is transcribed, yielding a primary miRNA precursor, which undergoes nuclear cleavage, resulting in a precursor miRNA. This precursor miRNA is transported and cleaved in the cytoplasm, creating a miRNA duplex containing the mature miRNA, and assembles into the RISC complex. The miRNA can base-pair with target mRNAs to preform gene silencing via mRNA cleavage, or, based on the level of complementarity between the miRNA and the mRNA target, perform translation repression (Awaiting permission: Winter et al. 2009) [81].

1.7.3 MiR-17-92 cluster

The miR-17-92 cluster is one of the best characterized miRNA clusters and is composed of six members which includes miR-17, miR-18a, miR-19a, miR-19b, miR-20a, and miR-92a. This cluster of related small non-coding RNAs is located on human chromosome 13 and has been verified to be upregulated in various types of cancers, including PCa [82, 83]. miR-17-92 cluster is expressed in embryonic cells and is considered fundamental in normal development [84, 85]. The term “cluster” can in some cases be used to indicate their genomic location and/or functional connection. Cluster as a term applies to a group of two or more miRNAs transcribed from the miRNA genes that are physically adjacent, transcribed in the same orientation, and also not disconnected by the miRNA or transcription unit from the opposite orientation [86].

Two paralogues of the miR-17-92 cluster exist in the human genome; miR-106a-363 (miR-106a, miR-18b, miR-20b, miR-19b-2, miR-92a-2 and miR-363) and the miR-106b-25 (miR-106b, miR-93 and miR-25) cluster. Collectively, miR-17-92 and its two paralogues encodes 15 miRNAs which can be grouped into 4 distinct "seed" families; miR-17, miR-18, miR-19, and miR-92, presented in Figure 9 [84, 85]. The miR-17-92 cluster along with its two paralogues clusters miR-106a-363 and miR-126b-25, act as oncogenes. The expression of these clusters stimulate cell proliferation, suppresses cancer cell apoptosis, and generates tumour angiogenesis [87, 88].

Even though an entire sequence of a miRNA can bind to a target, both computational and experimental evidence suggests that the nucleotides positioned between 2-7 inclusive from the 5' end of a miRNA, commonly known as the "seed" sequence, are the key determinants for both target determination and coupling [89-91]. Thus, miRNAs that shares seed sequences are anticipated to target strikingly overlapping set of genes, hence grouped in the same miRNA family [85, 91, 92].

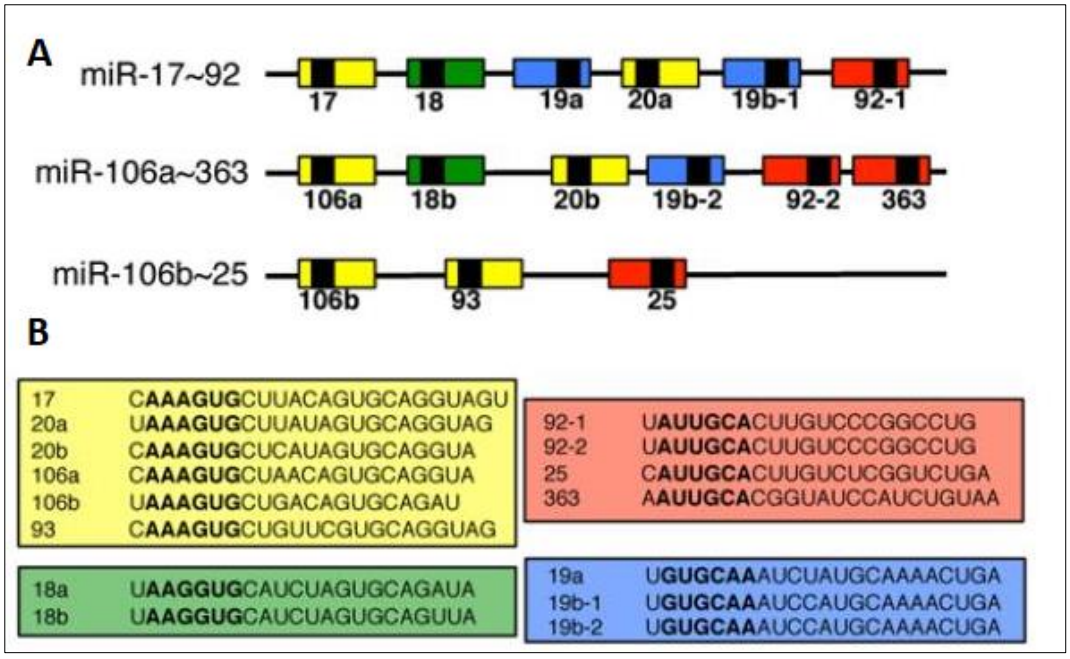

Figure 9: Members of the miR-17-92 family. (A) Figure presents a schematic presentation of the miR-17-92 family of miRNA clusters with its three members miR-17-92, miR-106a-363, and miR-106b-25. miRNAs sharing the same seed sequence are represented together with the same colour. (B) The miRNAs are grouped into four separate seed families, and sorted by colour, the four boxes show the mature miRNA sequences of the miRNAs encoded by the three clusters. Seed sequences are in bold. (Awaiting permission: Concepcion, 2013) [85].

The six mature miRNAs in the miR-17-92 cluster is implicated in several human cancers, targeting mRNAs which is involved in distinct pathways that either inhibit or promote carcinogenesis. Notably, oncogenic roles have been ascribed to the miR-17-92 cluster, including miR-17 and miR-20a, and both are reported to be overexpressed in primary PCa tissues compared to benign prostate tissue [93-96]. Furthermore, other studies have illustrated that abnormal expression of miRNAs, including miR-17 and miR-20a, are involved in outbreak, progression, and metastasis in PCa [52, 55, 97]. Nevertheless, the exact role of the miR-17-92 cluster regarding malignant progression in PCa is yet to be fully understood [93].

1.7.4 Locked nucleic acids (LNA™)

Locked nucleic acids (LNA™) is a modified RNA oligonucleotide whereas the ribose element is structurally linked to an extra bridge which connects the 2'-O and the 4'-C atoms, thus "blocking" the ribose in the 3'-endo conformation. This yields an ideal conformation for

Watson-Crick binding [52, 98]. The LNA™ oligonucleotides have the same nucleobases which can be observed in RNA and DNA, and by "locking" the molecules with the methylene bridge, the LNA™ is constrained, and therefore, when incorporated into an RNA or DNA oligonucleotide, makes the pairing with a complementary nucleotide strand more rapidly, furthermore, increasing the stability of the resulting duplex (Figure 10) [98-100].

Moreover, LNA™ oligonucleotides can be constructed shorter than the conventional RNA or DNA oligonucleotides and still retain a high melting temperature (Tm), which is important and favourable when the oligonucleotide is utilized to detect highly similar or small targets. Typical challenges in miRNA analysis is the highly varying GC-content (5-95%) [101], and small sizes of miRNAs, making it difficult for traditional methods. RNA or DNA based technologies may present both low robustness and high uncertainty due to low Tm of the oligonucleotide/miRNA duplex which will vary depending on the sequences GC content. Utilizing LNA™ enhanced oligonucleotides, these challenges can be reduced. Oligonucleotides with distinct duplex Tm can be designed by varying the content of the LNA™, regardless of the GC content of the miRNA [98-100]. Another advantage in utilizing LNA™ is their discriminatory capability, which can be used to distinguish between miRNA sequences that are closely related. [99, 102].

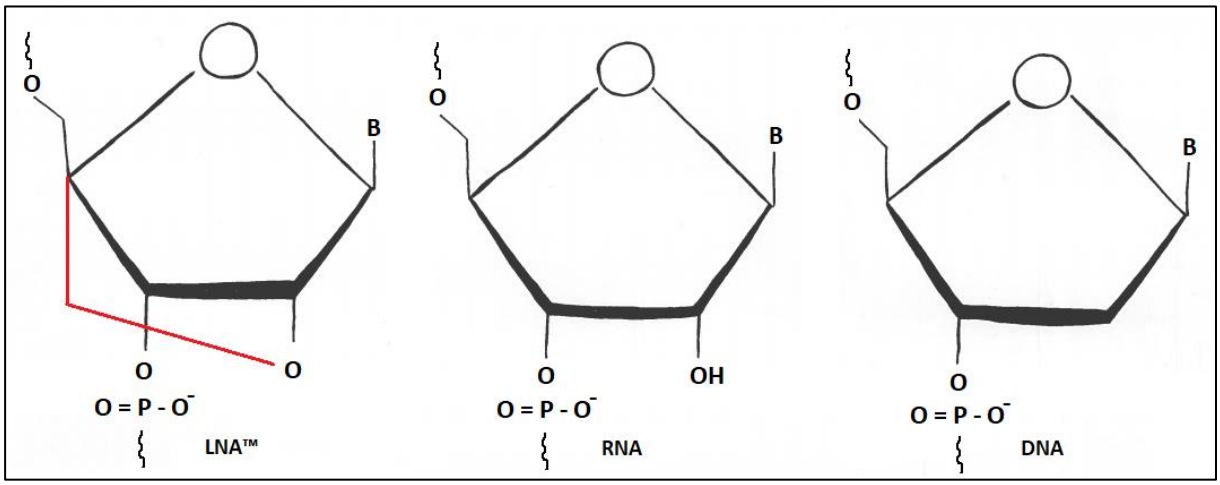

Figure 10: Structures of LNA™, RNA, and DNA. The ribose ring of LNA is “locked” by a methylene linkage between the 2’ oxygen and the 4’ carbon (B = Base), (Lise Martine Ingebriktsen, 2018).

1.8 The proliferation marker Ki-67

The proliferation marker Ki-67 is a human protein encoded by the *MKI67* gene, and is greatly associated with tumour cell proliferation, growth, and progression. Ki-67 indicates the proliferation rate of tumour cells, and has been correlated with progression, metastasis, and prognosis in various malignancies [103-107]. The expression of Ki-67 can be detected in the nucleus of tumour epithelial cells, and the expression of Ki-67 is widely used in routine histopathological investigation as a proliferation marker [108].

Since Ki-67 is involved in all active phases of the cell cycle (Figure 11), which includes G_1, S, G_2 and mitosis, and absent in resting cells (G_0 phase), makes it an exemplary marker in determination of tumour growth fraction [109]. The abundance of Ki-67 that is continuously present in the cell cycle, is regulated by a definite balance of degradation and synthesis, which is reflected by its relatively short half-life of 60 - 90 minutes. The pretherapeutic evaluation of the expression of Ki-67 is starting to become more essential in the assessment of tumour aggressiveness in addition to selecting the most sufficient treatment [110].

To date, the Ki-67 labelling index is the best studied marker in PCa in needle-biopsies [111-117]. Several findings have indicated that the Ki-67 labelling index shows great correlation with Gleason score in subsequent radical prostatectomy [114-116], diagnostic biopsies [111, 113], or both [112]. Moreover, some have found Ki-67 to be a biomarker for disease-free survival [112], cancer specific death after radical prostatectomy [117], and seminal vesicle invasion and postoperative biochemical failure [116]. Ki-67 is thoroughly distinguished at the molecular level and is widely used as a predictive and prognostic marker for cancer treatment and cancer diagnosis [110].

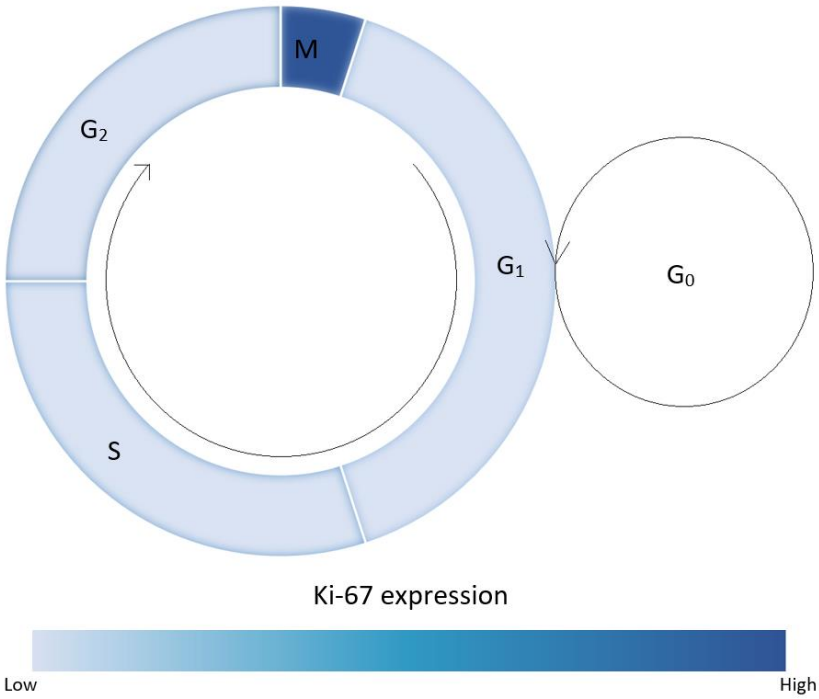

Figure 11: The expression of Ki-67 in various cell cycle phases. Cells express Ki-67 during G_1, S, G_2, and mitotic phases. Ki-67 is not expressed in G_0 phase. Ki-67 levels are low in G_1 and S phase and increases in level in the mitotic phase (M). Darker blue colour represents high expression of Ki-67, whereas light blue colour represents low expression of Ki-67. (Lise Martine Ingebriktsen, 2019).

1.9 *In situ* hybridization

In situ hybridization (ISH) is a strong and effective technique used for visualization at cellular level. The main goal of ISH is to detect the absence or presence of RNA or DNA sequences of interest, in addition to localize these sequences to precise chromosomal sites or cells. Furthermore, since the application of LNA™ probes, ISH has been used as a powerful tool to detect miRNAs at single-cell level, as well as to assess their physiologic function. Today, LNA™ probes are the most accepted in the practice of miRNA ISH, due to their increased specificity in target detection [118, 119].

The comprehensive ISH technique includes multiple steps; the formation of a labelled probe to assist subsequent detection, tissue fixation, increase accessibility of target nucleic acid by tissue pre-treatment, hybridization, several washing steps which removes non-hybridized probes, and lastly detection of the labelled probe, exposing the desired target location [120]. Some aspects need to be taken into consideration when choosing a probe for ISH, such as

the reproducibility of the method, the stability of hybrids, how efficiently the probe penetrates the tissue, and the specificity and sensitivity. Currently, Digoxigenin (DIG)-labeled RNA antisense probes are the most beneficial, popular, and effective choice for miRNA ISH. These DIG-labeled probes are widely used due to their high specificity and sensitivity, and these are stable for more than 12 months, making them ideal for continuing studies with minimal technical variation and high consistency [119, 121].

The ISH technique utilizes the specific strength of complementary nucleic acid molecules like DNA or RNA through hydrogen bindings between the bases Guanine, Cytosine, Adenine, and Tyrosine (Uracil in RNA), in the sugar-phosphate backbone. The sequences are read in correspondence to their positions of the sugar where the phosphate residues are attached 5' to 3'. This provides sequences to be precisely detected by utilizing a probe that is frequently recognized as an "antisense" reverse complementary sequence [120]. A big advantage in ISH detection of miRNAs, is the ability to both point out specific cellular locations and visualize the expression levels. The ISH technique has a good reproducibility, and it enables maximal use of tissues that is challenging to obtain, like clinical biopsies. However, this technique may offer time and cost requirements, and to a degree an expertise in result interpretation [118].

Figure 12 illustrates a simplified schematic presentation of a DIG-labeled ISH for miRNA detection. Normally, in manual ISH methods, mature miRNAs are demasked using proteinase K (serine protease). In automated ISH methods, used in this thesis, CC1 buffer (Citrate/EDTA) and high temperature (95 °C) are used to demask, which provides double-DIG labelled LNA™ probes to hybridize to the miRNA sequence. Following, the digoxigenin is recognized by an anti-DIG-antibody which is conjugated with Alkaline Phosphatase (enzyme). Alkaline Phosphatase converts the soluble substrates 4-nitro-blue tetrazolium (NTB) and 5-bromo-4-chloro-3’ indolylphosphate (BCIP) into a mix of alcohol and water insoluble dark-blue NBT-BCIP precipitates. Lastly, to give a better histological resolution, red nuclear counterstain is applied [118, 119, 122].

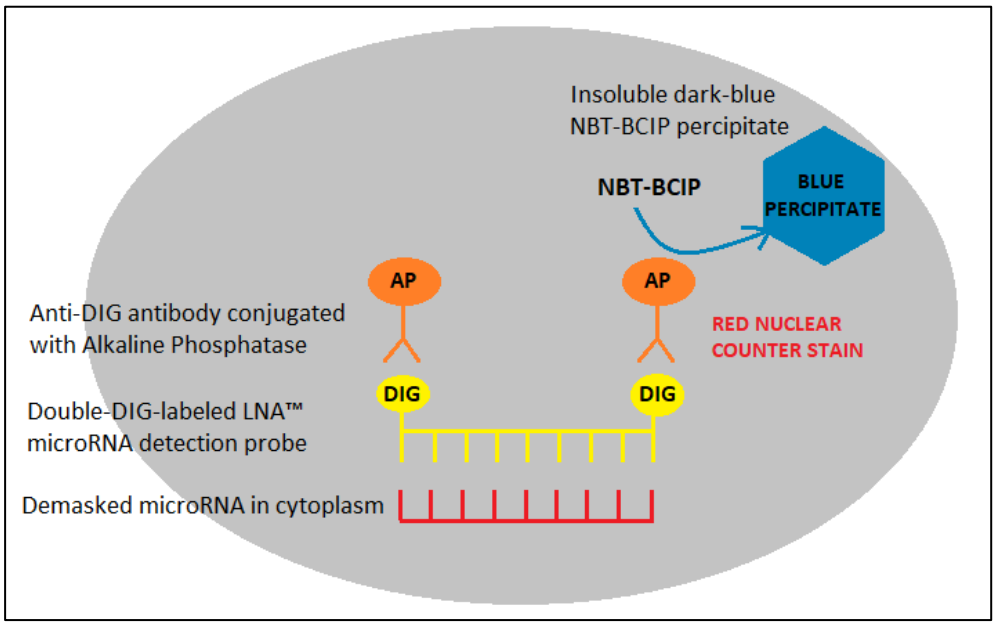

Figure 12: In situ hybridization analysis with chromogenic detection. Mature miRNA in the cell cytoplasm is demasked, providing double-DIG labelled LNA™ (coloured yellow) probes to hybridize to the miRNA sequence. Subsequently, digoxigenin can be recognized by an anti-DIG-antibody that is conjugated with the Alkaline Phosphatase enzyme (coloured orange). The enzyme converts the soluble substrates NBT and the BCIP into a water and alcohol insoluble dark-blue NBT-BCIP precipitates (coloured blue). The nuclear is coloured with a red counter stain. Abbreviations; NBT: 4-nitro-blue tetrazolium, BCIP: 5-bromo-4-chloro-3' indolylphosphate, AP: Alkaline Phosphatase, DIG: Digoxigenin. (Lise Martine Ingebriktsen, 2019).

1.10 Aims

The aim of this thesis is to examine the prognostic role of miR-17-5p and miR-20a-5p in PCa tissue and their potential role as biomarkers. In addition, correlate the expression level of miR-17-5p and miR20a-5p with the expression of the proliferation marker Ki-67. In detail:

- Examine the *in situ* tissue distribution of the microRNAs miR-17-5p and miR-20a-5p in untreated prostatectomy specimens. Furthermore, correlate these miRNAs to the proliferation marker Ki-67.
- Retrospectively evaluate the prognostic impact of marker expression on the following clinical outcomes: Biochemical failure (BF), Clinical failure (CF), and Prostate cancer death (PCD) by performing univariate- and multivariate analyses.

2 Materials and Methods

2.1 Patients

This study includes a large PCa cohort (n = 671) retrospectively collected from the archives of the Departments of Pathology at the University Hospital of North Norway (UNN) (n = 267), St. Olav Hospital/Trondheim University Hospital (St. Olav) (n = 341), and Nordlandssykehuset Bodø (NLSH) (n = 63), between 1995 and 2005. 131 patients of the original cohort were excluded, resulting in 535 qualified patients with complete follow-up data and tissue blocks for re-evaluation (Figure 13).

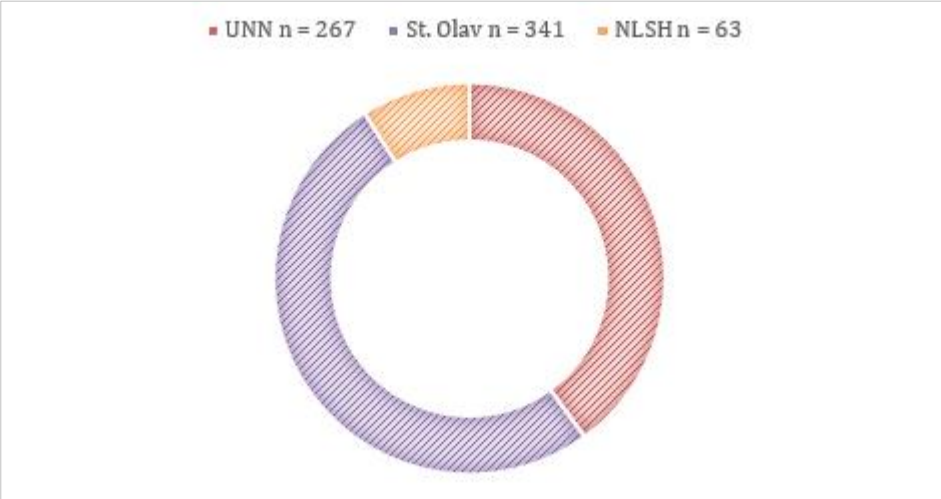

Figure 13: Patients included in this study. Diagram presenting the total number of patients included from the archives of the Departments of Pathology at the University Hospital of North Norway (UNN), St. Olav Hospital (St. Olav), and Nordlandsykehuset Bodø (NLSH). (Lise Martine Ingebriktsen, 2019).

2.2 Tissue preparation and tissue microarray construction

Tumour tissues consists of formalin-fixed, paraffin embedded (FFPE) blocks of prostate tissue which are beneficial as collection of tissues from patients with definite diseases. In this study, tissues from 535 PCa patients was used. Tissue matrix technology allows investigation of multiple tissue samples from several different patients simultaneously.

The Tissue microarrays (TMAs) are assembled utilizing a tissue arraying instrument (Beecher Instruments, Silver Springs, MD, USA). An experienced pathologist (ER) identified and marked representative prostate specimen areas with tumour epithelial cells (TE), tumour associated stromal cells (TS), in addition to normal epithelial, and normal stromal cells (NE and NS respectively). An illustration on such representative areas marked on PCa tissue are presented in Figure 14 and 15. Cores were harvested from the marked areas from the corresponding FFPE tissue blocks by using a 0.6 mm diameter needle. This provides small cylinders of tissue samples being removed from the donor furthermore added to an empty recipient paraffin block corresponding to pre-defined coordinated pattern.

A total of twelve matrices were made, and it was also done equivalent for both normal epithelial and stromal tissue within the same cancer patient. Additionally, TMA containing tissue from PCa free patients were made. Several 4 µm (1 µm = 0.001 mm) sections were cut by an experienced biomedical laboratory scientist operating a Micron Microtome (HM355S; Thermo Fisher Scientific Life Sciences, Waltham, MA), ultimately attached to slides and sealed with paraffin. Such tissue matrix blocks serve as standardized collections of tissues from all patients included.

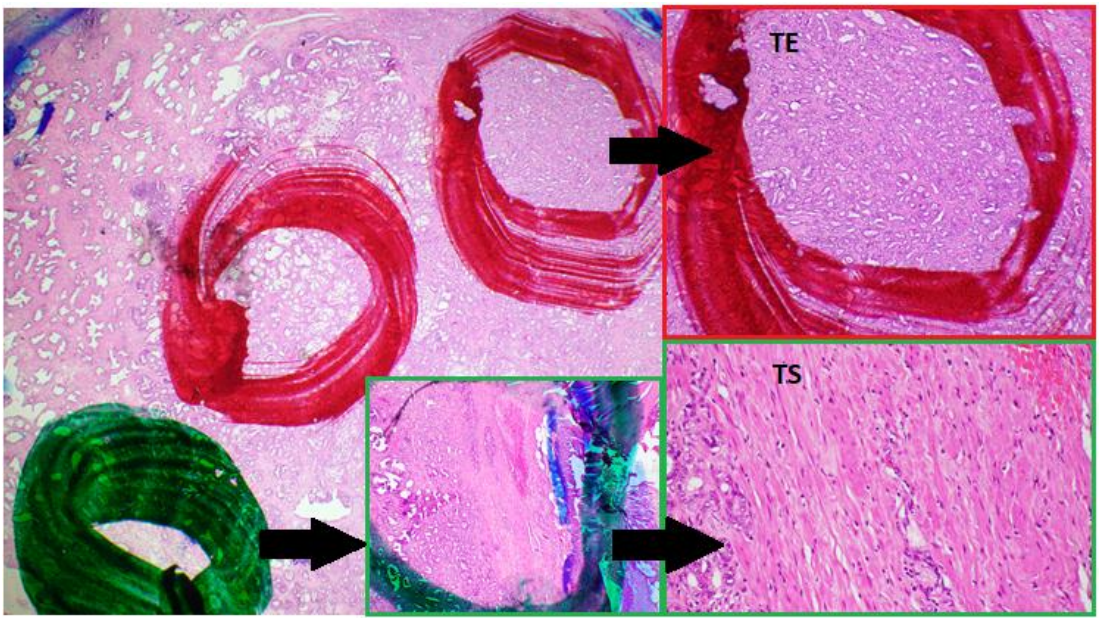

Figure 14: Representative prostate specimen areas. Figure shows tumour epithelium (red) and tumour stromal (green) areas marked on a prostate gland histology slide. Abbreviations; TE: tumour epithelium, TS: tumour stroma. (Picture: Elin Richardsen).

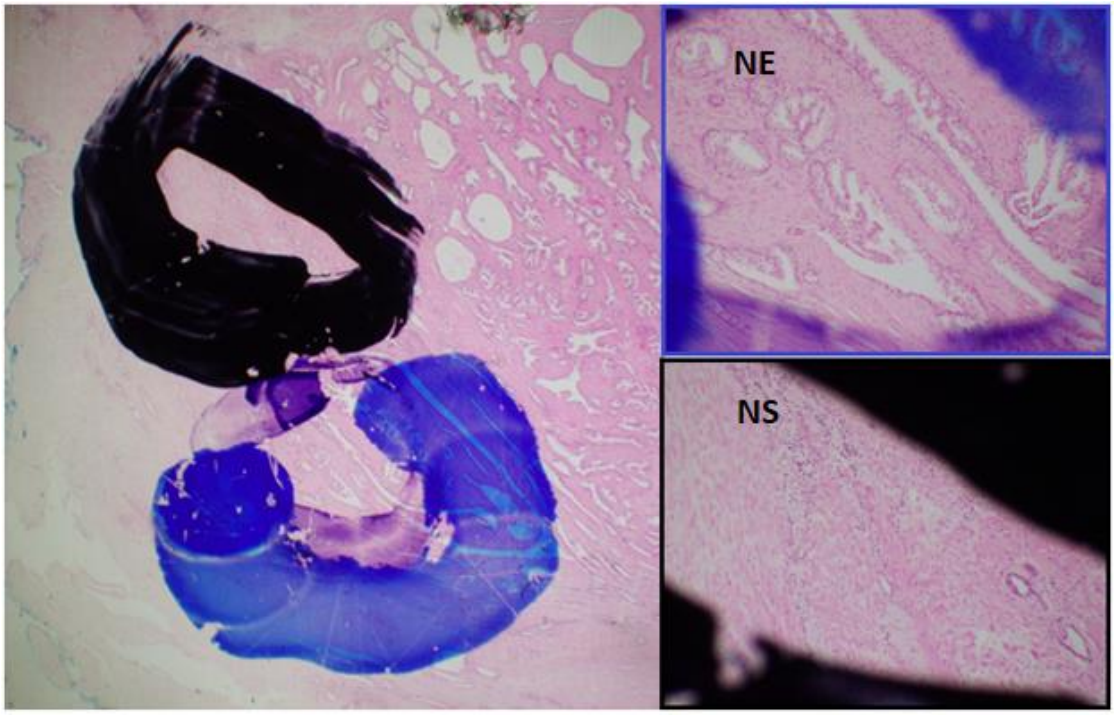

Figure 15: Representative prostate specimen areas. Figure shows normal epithelium (blue) and normal stromal (black) areas marked on a prostate gland histology slide. Abbreviations; NE: normal epithelium, NS: normal stroma. (Picture: Elin Richardsen).

2.3 Preparation and optimization of the miRCURY LNA™ microRNA Detection probes

In situ hybridization was performed on Ventana Discovery Ultra instrument (Ventana Medical Inc, Arizona, USA). Detection reagents and buffers were supplied from ROCHE (Basel, Switzerland), and the Danish company Exiqon (Vedbaek, Denmark) supplied the miRCURY LNA™ microRNA Detection probes and controls; hsa-miR-17-5p, (No. 619852-360), hsa-miR-20a-5p, (No. 611011-360), positive control (U6 hsa, No. 160010126), and negative control (scrambled-miRNA, No. 157057117). These LNA™ oligonucleotides offers remarkably increased affinity for its complementary strand, compared to the traditional DNA or RNA oligonucleotides.

The probes are shipped at room temperature, and immediately after receipt, the oligonucleotides are stored aliquoted in stock concentrations at – 20 °C protected from light. These conditions provide the probes to be stable for at least 6 months. Detection require re-suspension before first use. This is a relatively standard procedure which includes spinning

down the tubes briefly to pellet the probes. Furthermore, the probes are re-suspended by adding 40 µl nuclease-free Elix water to the tube to a final stock concentration of 25 µm, and lastly this stock concentration of 25 µm was diluted to a 100 nM stock.

In this study, the optimal stock concentration for each miRNA was calculated utilizing the Oligo dilution calculator [123]. The Oligo dilution calculator is a tool used to determine how much water and buffer to be added to a stock solution to obtain a desired concentration. The stock concentration value (nM), stock volume (µL), and the desired target concentration (nM) was entered in the calculator. Results for the two probes are presented in Table 2. Results for the controls U6 and scramble miR are presented in Table 9 in the appendix. The buffer used in these calculations was a buffer provided by Exiqon called microRNA ISH buffer, which is a hybridization buffer specifically used on LNA™ probes, typically operating with a 1:1 concentration. While preparing LNA™ probes, working RNase-free is highly important. All equipment used, including buffers in instruments were RNase-free.

Table 2: Table presenting values from the Oligo Dilution Calculator, delivered by Qiagen. Stock concentration, stock volume and desired target concentration were entered for the probes miR-17-5p and miR-20a-5p, to calculate water/buffer ratio (1:1), and total volume.

Probe	Stock concentration	Volume	Target concentration	Water/buffer	Total volume
miR-17-5p	100 nM	360 µL	20 nM	1440 µL	1800 µL
miR-20a-5p	100 nM	850 µL	50 nM	850 µL	1700 µL

Positive and negative tissue controls for the two probes were comprised of a stained TMA multi-organ block, whereas the controls comprised 12 various organs with both tumour and normal tissues. Hybridization, stringent wash temperatures and concentrations were optimized for each probe. To minimize the risk of RNA degradation, Elix RNAse-free water was used during the optimization process.

Probe concentrations and unmasking pre-treatments were tested on one TMA multi-organ block to optimize the detection method. Hybridization temperatures for the controls and each probe was tested with the recommended RNA melting temperature (Tm) as a guideline, listed in the product data sheet (Exiqon, QIAGEN). Commonly in the case of miRCURY LNA™ detection probes, RNA Tm is approximately around 80 °C. miR-17-5p, and miR-20a-5p, both had distinct RNA Tm; 91°C and 82 °C respectively. When calculating the optimal hybridization temperature for each probe, one usually begins with the recommended estimation of 30 °C below the listed RNA Tm as starting point. Note: Testing was done on TMA multi control tissue block representing different type of cancers and normal tissue. The final hybridization temperature was ultimately tested on both prostate and breast cancer TMA controls.

In the case of miR-17-5p, the RNA Tm was relatively high (RNA Tm 91 °C), and the testing started with 61 °C, which resulted in un-satisfactory and diffuse staining. Since the recommended RNA Tm did not achieve favourable staining, both higher and lower hybridization temperature was tested. No staining was detected at 65 °C, and only weak staining was detected at 50 °C. Consequently, by choosing an intermediate at 54 °C, an optimal hybridization temperature was achieved, which provided good and strong staining. Following, miR-20a-5p began with Tm 52 °C (RNA Tm 82 °C). This gave weak and unspecific overall staining, thus trying higher and lower temperatures, 56 °C and down to 40 °C. It should be mentioned that miR-20a-5p ended up with a considerable high probe concentration to achieve moderate staining, since lower probe concentration combined with lower hybridization temperature failed to provide good staining. Higher hybridization temperature served no good, thus early eliminated as an option. Although the final Tm of 40 °C did not show as strong overall staining compared to miR-17-5p, no further testing was done due to the already high probe concentration, where it was decided that higher probe concentration presumably would not make a significant difference. The sensitivity level of the ISH method was ensured by utilizing U6 snRNA control probe at 1.5 nM concentration. Nuclear signal at concentrations between 0.1-2.0 nM for U6 was considered optimal sensitivity. Additionally, U6 indicated low degree of RNA degradation by visualizing strong

nuclear staining by light microscope. Scramble miR negative control probe showed no unspecific positive staining in prostate TMA cores, illustrated in Figure 16.

Table 3: Table presenting the chosen hybridization temperature used for each LNA™ oligonucleotide, and the recommended RNA Tm melting temperature given in the product data sheet provided by Exiqon. The Tm is given as a guideline to calculate a more precise hybridization temperature, which should be estimated 30 °C below RNA Tm.

Probe	**RNA Tm (°C)**	**Hybridization temperature (°C)**
miR-17-5p	91	54
miR-20a-5p	82	40
U6 hsammumo	84	55
Scramble-miR	87	57

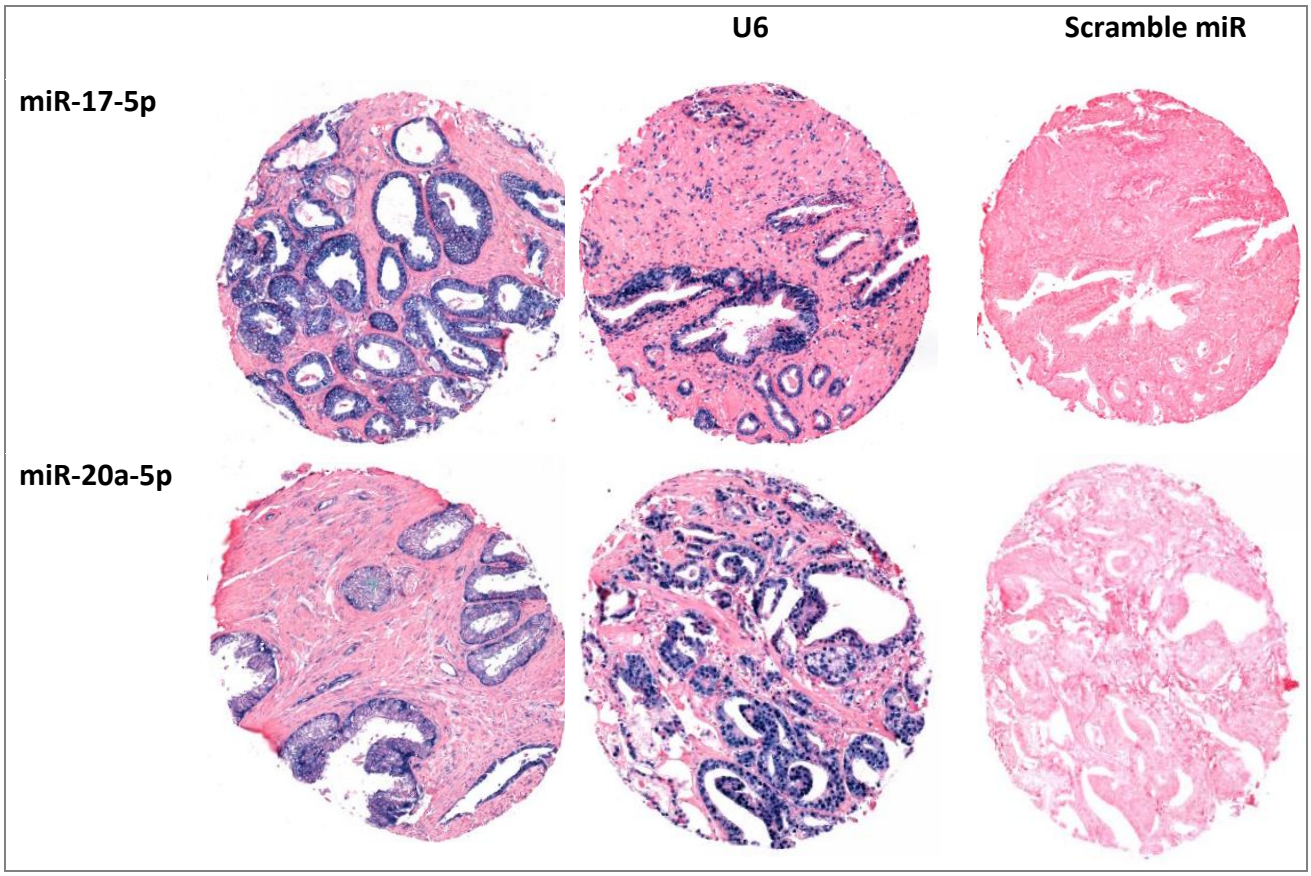

Figure 16: Figure representing a visualization of the TMA cores, as result from the controls U6 and Scramble miR in testing sensitivity level of the ISH method. (Lise Martine Ingebriktsen, 2018).

2.4 ISH procedure

The 4 µm sections was mounted onto SuperFrost Plus™ Adhesion slides, which are slides used with intent to minimize tissue loss during the staining procedure. The sections were incubated overnight at 60 °C to attach the tissue to the Super Frost Plus slides, and to melt away the paraffin. Protocols and labels were made using the Ventana data program (SN 312464 VSS v. 12.4 Build 15110.1). To ensure that the reagents were properly distributed, and providing the slides from drying, all incubations in Discovery Ultra were added Liquid Coverslip Oil (Roche, 5264839001). Details of the ChromoMap™ Blue kit, anti-DIG, and antibody block utilized is presented in Table 10 in the appendix.

The ISH protocol started off by deparaffinization, where the slides were warmed up to 68 °C ahead of three 12-minute deparaffinization cycles. Subsequently, a pre-treatment which is important for tissue integrity and morphology followed, by warming the slides to 95 °C,

followed by a 4 minutes incubation. This provides target unmasking with the intent to loosen and disengage cross linking effect which occurs in formalin fixation. Furthermore, the slides went through target unmasking for 40 minutes at 95 °C with Cell Condition 1 (CC1 buffer) (Roche, 6414575001). After the last CC1 step, the probes were applied manually: miR-17-5p (Exiqon, 619852-360), miR-20a-5p (Exiqon, 611011-360), scramble miR (Exiqon, 99004-15) negative control probe, and U6 (Exiqon, 99002-15) positive control probe.

The following step in the protocol was denaturation and hybridization. By heating the slides to 90 °C with an 8 minutes incubation, it engages the process of straightening out the typical RNA “hairpin” structure, providing a straight line so that the probe more easily can bind to its target, which is important in order to perform hybridization. To create "probe-target" hybrids and reform the hydrogen bonds by nucleic acid pair matching, the slides were warmed up from extended low temperatures and incubated in 60 minutes. Hybridization with probes was performed at 54 °C for miR-17-5p, 40 °C for miR-20a-5p, 57 °C for scramble miR, and 55 °C for U6. To ensure specific probe-target hybrids and removal of non-specific hybrids and unbound probes, stringency washes was performed 2 x 8 min with 2.o X Ribo Wash, and SSPE buffer with the same temperatures as used under hybridization for each probe mentioned above.

The last steps in the ISH protocol was detection. Antibody block (Roche, 5268869001) which removes non-specific binding from the immunological reagents, was applied following a 16 minutes incubation, subsequently followed by adding Alkaline phosphate conjugated anti DIG (Anti-DIG-AP multimer, Roche 07256302001) with 20 minutes incubation. The probes are DIG-labeled in both the 3’ and 5’ which binds to its specific miRNA target, and the anti-DIG complex binds to the DIG-labeled ends located at both ends of the probe sequence. After rinsing substrate enzymatic reactions was carried out with NBT/BCIP (ChromoMap Blue kit, Roche, 526661001) for 60 minutes. The ChromoMap Blue kit reacts with AP in the anti-DIG complex, resulting in the detection of the miRNA. Sections were again rinsed and counterstained 4 min with Red Stain II (Roche, 5272017001). Ultimately, the slides were collected from the Ventana Discovery Ultra instrument and washed manually in tap water, followed by dehydration performed by increasing gradients of ethanol solutions to Xylene.

Finally, sections were mounted with Histokitt mounting medium (Assistant-Histokitt 1025/250 Sondheim/Rohen Germany).

2.5 Scoring of expression and interclass correlation

All sections were scanned on a Panoramic 250 Flash III Device (3DHistech, Budapest, Hungary), and the images were visualized using CaseViewer 2.2 64-bit version (3DHistech, Budapest, Hungary). CaseViewer, functioning as a digital microscope, is designed to provide a unique support in histopathological diagnosis and examination processes. All tissue samples were scored semi-quantitatively by one uro-pathologist (ER), and a trained investigator/student (LMI) independent of each other and blinded to any clinical or pathological information, (Ki-67 was scored by ER and LBT). In case of discrepancy (score difference > 1), the cores were re-examined, and a consensus reached. Consequently, all reported marker expressions are based on two individual evaluations of the tissue cores. Marker expressions were evaluated in following PCa compartments for all miRNAs: Tumour Epithelium (TE) and Tumour Stroma (TS), presented in Table 4.

Table 4: PCa compartments evaluated in the miRNAs miR-17-5p and miR-20a-5p. Intensity and density were scored in tumour epithelium and tumour stroma respectively.

Biomarker	Tumour epithelium	Tumour stroma
miR-17-5p	Intensity	Density
miR-20a-5p	Intensity	Density

The two miRNAs in each tissue compartment were given a score between 0 – 3, where 0 = 0%, 1 = 1 - 20%, 2 = 21 - 49%, 3 = > 50%, representing the percentage of positive cells in the examined compartment (Figure 17). If a core was either considered of insufficient quality to score, or missing, a core was given the score “missing” (4).

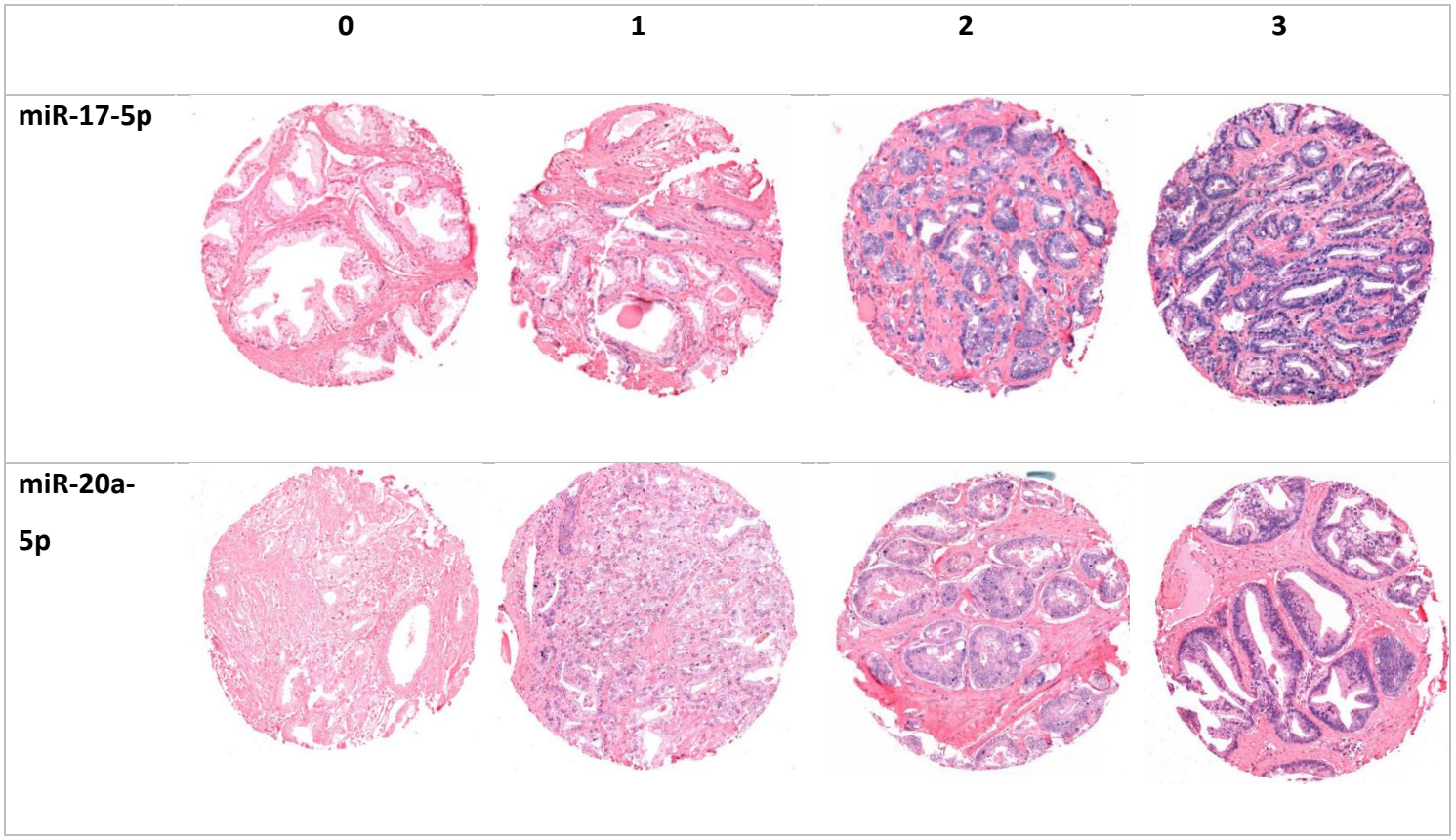

Figure 17: Figure showing cores which represents the range of scores 0-3 in the scoring evaluation of the miRNAs miR-17-5p and miR-20a-5p. (Lise Martine Ingebriktsen, 2018).

Intraclass correlation coefficient (ICC) is a commonly used reliability index in various analyses. Reliability is frequently defined as the extent to which a test or experiment or measurements can be replicated, meaning that it reflects both the agreement between measurements, and the degree of correlation. Ronald Aylmer Fisher was the first to introduce ICC in 1954 [124], and since, ICC have been broadly used in traditional care medicine to assess test-retest, intra- and interrater reliability. These types of assessments are elemental to classic evaluations, because without these, one cannot draw reasonable conclusions nor achieve confidence from the measurements [125].

Importantly, one must choose the correct ICC form for interrater reliability studies. In this case, the "two-way mixed" model was chosen since the selected raters (ER, LMI) were the only raters of interest, hence, the results only displayed the reliability of the specific raters that were involved in the given reliability experiment. Moreover, the definition selected in this case was "absolute agreement", whereas this concerns if dissimilar raters designate the

same score to the same subject. ICC were performed in SPSS, version 25 (SPSS Inc., Chicago, IL, USA). Values greater than 0.90, between 0.75 and 0.9, between 0.5 and 0.75, and less than 0.5 were regarded as excellent, good, moderate, and poor reliability, respectively.

2.6 Statistics

All statistical analysis including univariate and multivariate analyses was performed using IBM SPSS version 25 (SPSS Inc., Chicago, IL, USA). The statistical significance of the Kaplan-Meier survival curves was assessed by the log-rank test in univariate analysis. Biochemical failure, clinical failure, and prostate cancer death (BF, CF, PDC), were considered end points in the survival analyses. Significant variables from the univariate analysis was entered into multivariate analysis by backward stepwise cox regression. P value < 0.05 was considered statistically significant for all analyses. Figure 18 illustrates a flow chart showing an overview of the statistical analysis performed, and details around the end points considered in the survival analyses.

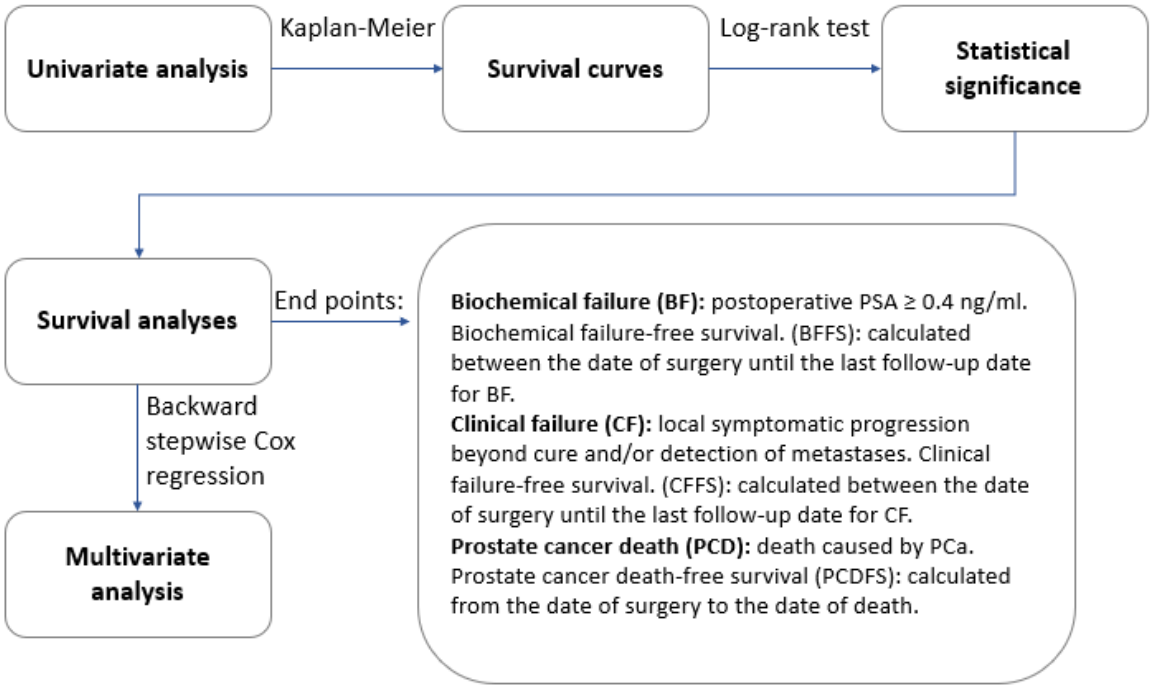

Figure 18: Flow chart presenting an overview of the statistical analysis performed in this thesis. Statistical significance of survival curves was assessed by the log-rank test. End points in the survival analyses were biochemical-, clinical failure and prostate cancer death. Significant variables from univariate analyses was entered into multivariate analysis. (Lise Martine Ingebriktsen, 2019).

3 Results

3.1 Patient characteristics

An overview of the patients' clinicopathological characteristics are presented in Table 5. Median age at surgery was 62 (range: 47-75), median tumour size was 20 mm (range: 2.0-50), and median PSA was 8.8 (range: 0.7-104). At the last follow-up (Dec 2015), 37% of the patients underwent BF, 11% underwent CF, and 3.4% of the patients died due to PCa.

Table 5: Patient characteristics and clinicopathological variables as predictors of biochemical failure free survival, clinical failure-free survival, and disease-specific survival (univariate analysis; log-rank test), No = 535. Significant p-values is highlighted (p ≤ 0,05).

Characteristic	Patients (n)	Patients (%)	BF (n=200)		CF (n=56)		PCD (n=18)	
			5-year EFS (%)	**P**	**10-year EFS (%)**	**P**	**10-year EFS (%)**	**P**
Age				0.237		0.038		0.404
< 65 year	357	67	77		94		98	
≥ 65 year	178	33	70		91		98	
Preop. PSA				**<0.001**		**0.029**		**0.003**
PSA < 10	308	57	81		95		99	
PSA > 10	221	42	68		89		97	
Missing	6	1						
pT-stage				**<0.001**		**<0.001**		**0.001**
pT2	374	70	83		97		99	
pT3a	114	21	61		87		98	
pT3b	47	9	43		74		91	
pN-stage				**<0.001**		**<0.001**		**<0.001**
NX	264	49	79		96		99	
N0	268	50	72		90		97	
N1	3	1	0		33		67	
PNI				**<0.001**		**<0.001**		**<0.001**
No	401	75	80		96		99	
Yes	134	25	60		83		95	
Tumour size				**<0.001**		**0.002**		0.085
< 20 mm	250	47	83		96		99	
≥ 20 mm	285	53	68		90		97	

PSM				**0.049**		0.198		0.843
No	249	47	81		90		98	
Yes	286	53	69		96		98	
Apical PSM				0.063		0.427		0.128
No	381	71	82		96		99	
Yes	154	29	57		85		96	
Non-Apical PSM				**<0.001**		**<0.001**		**0.022**
No	381	71	82		96		99	
Yes	154	29	57		85		96	
LVI				**<0.001**		**<0.001**		**<0.001**
No	492	92	77		95		99	
Yes	43	8	47		70		90	
Surg. Proc.				0.466		0.308		0.965
Retropubic	435	81	77		92		98	
Perineal	100	19	68		95		99	
Gleason				**<0.001**		**<0.001**		**<0.001**
Gr. gr. 1 (3+3)	183	34	83		98		99	
Gr. gr. 2 (3+4)	219	41	77		94		99	
Gr. gr. 3 (4+3)	81	15	70		90		96	
Gr. gr. 4 (4+4)	17	3	58		86		94	
Gr. gr. 5 (>8)	35	7	36		65		91	

Abbreviations: BF = biochemical failure; CF = clinical failure; PCD = prostate cancer death; PCa = prostate cancer; EFS = event free survival; LVI = lymphovascular infiltration; NR = not reached; PNI = Perineural infiltration; Preop = preoperative; PSA = Prostate specific antigen; PSM = Positive surgical margin; Surgical proc = surgical procedure; Gr. gr.= grade group: 1 (≤6), 2 (3+4), 3 (4+3), 4 (4+4), 5 (>8).

3.2 MicroRNA expression

The expression of miR-17-5p and miR-20a-5p was located in both epithelial and stromal cells, and it was detected both nuclear and cytoplasm staining. For both probes, ISH staining was detected in the majority of tissue cores, including tumour and normal tissue compartments. The positive control U6 showed strong nuclear staining in nucleoli in the epithelium and nuclei in cells in the cytoplasm. Scramble miR negative control probe showed no unspecific positive staining in the prostate TMA cores. High miR-20a-5p score (TS) was significant associated with reduced survival for biochemical failure. Low score was defined as mean < 3.9 and high score as mean > 3.9. High miR-20a-5p score (TE) was significant associated with reduced survival for biochemical failure. Low score was defined as median < 4 and high score as median > 4. For miR-17-5p (TE), low score was defined as mean < 5.2 / median < 5.5, and high score as mean > 5.2 / median > 5.5.

3.3 Correlations

Correlations were explored between the expression of miR-17-5p, miR-20a-5p and clinicopathological variables. The results showed a significant correlation between miR-17-5p in TE (mean) and perineural infiltration ($r = 0.12$, $p = 0.005$). There was also significant correlation between miR-20a-5p and perineural infiltration for both TE ($r = 0.14$, $p = 0.002$) and TS ($r = 0.17$, $p = <0.001$). Correlation between the miRNAs and Ki-67 was also investigated. The results showed significant correlation between miR-17-5p in TE and Ki-67 for both cut-offs mean ($r = 0.18$, $p = <0.001$), and median ($r = 0.22$, $p = <0.001$). The results also showed significant correlation between miR-20a-5p in TE (median) and Ki-67 ($r = 0.11$, $p = 0.018$). Correlations were significant at the 0.01 level (2-tailed). Regarding ICC, good reliability values was achieved (0.75-0.85).

3.4 Univariate analysis

Results from the univariate analyses of clinicopathological variables and miRNAs and their association to the following outcome measures BF, CF, PCD, are presented in Table 5. The significant prognostic clinicopathological factors for BF were Gleason grade group ($p < 0.001$), lymphovascular infiltration ($p < 0.001$), non-apical PSM ($p < 0.001$), positive surgical margin ($p = 0.049$), tumour size ($p < 0.001$), perineural infiltration ($p < 0.001$), pN-stage ($p < 0.001$), pT-stage ($p < 0.001$), preoperative PSA ($p < 0.001$). Significant prognostic factors for CF were Gleason grade group ($p < 0.001$), lymphovascular infiltration ($p < 0.001$), non-apical PSM ($p < 0.001$), tumour size ($p = 0.002$), perineural infiltration ($p < 0.001$), pN-stage ($p < 0.001$), pT-stage ($p < 0.001$), preoperative PSA ($p = 0.029$), and age ($p = 0.038$). Significant prognostic factors for PCD were Gleason grade group ($p < 0.001$), lymphovascular infiltration ($p < 0.001$), non-apical PSM ($p = 0.022$), perineural infiltration ($p < 0.001$), pN-stage ($p < 0.001$), pT-stage ($p = 0.001$), and preoperative PSA ($p = 0.003$).

Regarding the miRNAs, both miRNAs had associations between expression in either tumour epithelium (TE) and/or tumour stroma (TS) in BF. In each univariate analysis, both mean and median cut-offs were tested. High expression of miR-17-5p in TE (median = 5.5, mean = 5.2) was associated with BF ($p = 0.033$, and $p = 0.010$ respectively). No significant association was found in TS, nor the other endpoints. In the case of miR-20a-5p, high expression in TE (median = 4) and TS (mean = 3.9) was associated with BF ($p = 0.019$, and $p = 0.042$ respectively), although not with CF or PCD. Kaplan-Meier survival curves representing miR-17-5p expression in TE (mean and median), in addition to miR-20a-5p expression in TS and TE is presented in Figure 19.

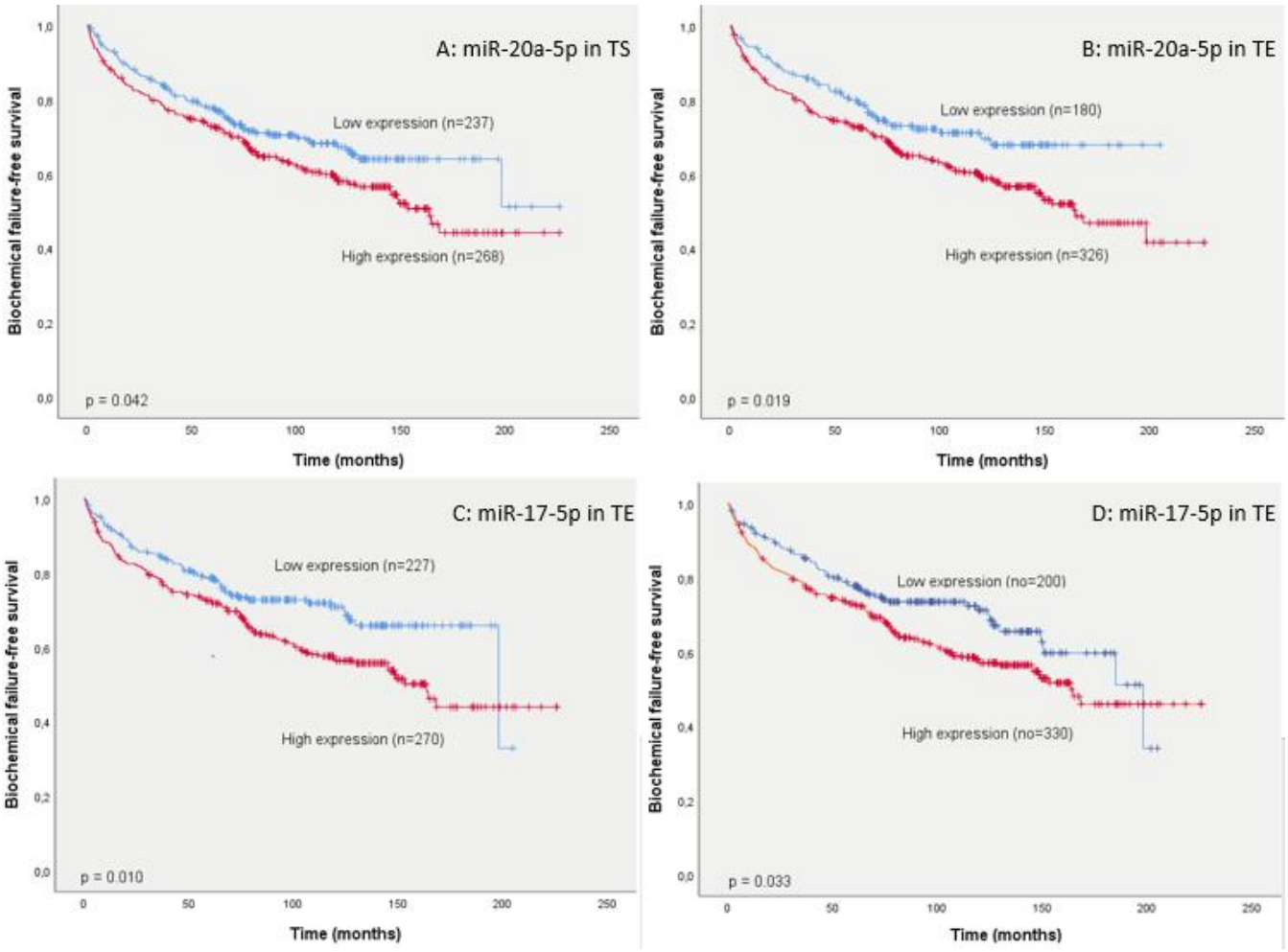

Figure 19: Kaplan-Meier curve presenting significant results from univariate analysis. The Kaplan-Meier curves show the amount of PCa patients (n = 535) survival without biochemical failure over time, distributed by high and low miRNA scoring in tumour epithelium and tumour stroma. A reduction of biochemical failure-free survival was demonstrated for patients with a high expression of miR-20a-5p in tumour stroma (A) and tumour epithelium (B), and for patients with a high expression of miR-17-5p in tumour epithelium (C and D). Significant p-value shown in lower left corner (threshold $p \leq 0.05$). Abbreviations; TE: tumour epithelium, TS: tumour stroma. (Lise Martine Ingebriktsen, 2019).

3.5 Multivariate analysis

Only significant outcomes were included in the multivariate analysis. Results from multivariate analysis are presented in Table 6. The table displays multivariate analysis for miR-17-5p in TE (mean and median), Ki-67 in TE (≥ 1.43) [126], TE (median) and TS (mean) for miR-20a-5p for BF.

High expression of miR-20a-5p in TE (median), (HR: 1.56, 95% CI: 1.08-2.26, p = 0.018) and Ki-67 in TS (HR: 1.55 95% CI: 1.12-2.13, p = 0.008) came out as significant independent prognosticators for BF. Clinicopathological variables significant for BF; preoperative PSA (HR: 1.15, 95% CI: 1.09-2.11, p = 0.014), positive surgical margin (HR: 1.60, 95% CI: 1.13-2.26, p = 0.008), pT stage pT3a, pT3b (HR: 1.58 95% CI: 1.22-2.05, HR: 0.59 95% CI: 0.36-0.98), and perineural infiltration (HR: 1.51 95% CI: 1.05-2.17, p = 0.025). Neither miR-20a-5p (TS, mean), nor miR-17-5p (TE, mean or median) came out significant in the multivariate analysis.

Table 6: Results from the multivariate analysis. The table presents the results from Cox regression analysis (backward stepwise model).

Characteristics	**No**	**Biochemical failure**	
		HR (95% CI)	**P**
Age			NS
< 65	280		
> 65	135		
Preop PSA			**0.014**
PSA < 10	238	1	
PSA > 10	177	1.15 (1.09-2.11)	
Missing			
Gleason grade group			NS
1 (3+3)	128		
2 (3+4)	245		
3 (4+3)	68		
4 (4+4)	15		
5 (>9)	27		
Positive surgical margin PSM			**0.008**
No	298	1	
Yes	177	1.60 (1.13-2.26)	
Tumour size			NS
< 20 mm	181		
> 20 mm	234		
pT stage			**< 0.001**
pT2	294	1	

pT3a	88	1.58 (1.22-2.05)	
pT3b	33	0.59 (0.36-0.98)	
Perineural infiltration			**0.025**
No	312	1	
Yes	103	1.51 (1.05-2.17)	
miR-20a-5p in epithelium (median)			**0.018**
Low expression	149	1	
High expression	266	1.56 (1.08-2.26)	
Ki-67			**0.008**
Low expression	249	1	
High expression	166	1.55 (1.12-2.13)	
miR-20a-5p in stroma (mean)			NS
Low expression	203		
High expression	212		
miR-17-5p in epithelium (mean)			NS
Low expression	145		
High expression	270		
miR-17-5p in epithelium (median)			NS
Low expression	199		
High expression	216		

Abbreviations: HR: Hazard ratio, CI: Confidence interval, PSA: Prostate specific antigen, PSM: Positive surgical margin, NS: Not significant, No: Number, P: p-value). In addition to the miRNAs and Ki-67, the table shows independent prognosticators for patient outcome in PCa patients (n = 535). Significant p-values are in bold (threshold p = ≤0.05).

Tables 7 and 8 presents the results from Cox regression analysis (backward stepwise model) for miR-20a-5p (TE and TS) for biochemical failure, in addition to other remaining independent prognosticators for patient outcome in PCa patients (n = 535). Significant p-values are in bold (threshold p = ≤0.05).

Table 7: Results from the multivariate analysis for miR-20a-5p expression in TE (median).

Characteristics	**No**	**Biochemical failure**	
		HR (95% CI)	**P**
Age			NS
< 65	334		
> 65	166		
Preop PSA			**0.007**
PSA < 10	292	1	
PSA > 10	208	0.66 (0.49-0.86)	
Missing			
Gleason grade group			**0.038**
1 (3+3)	169	1	
2 (3+4)	205	1.19 (0.26-5.47)	0.821
3 (4+3)	77	2.02 (0.45-9.23)	0.361
4 (4+4)	17	2.25 (0.45-11.1)	0.322
5 (>9)	32	2.63 (0.58-12.0)	0.211
Positive surgical margin PSM			**<0.001**
No	366	1	
Yes	134	0.55 (0.39-0.76)	
Tumour size			NS
< 20 mm	235		
> 20 mm	265		
pT stage			**<0.001**
pT2	357	0.98 (0.63-1.51)	0.921
pT3a	100	1.59 (0.83-3.02)	0.159
pT3b	43	0.60 (0.38-0.99)	**0.036**
miR-20a-5p in epithelium (median)			**0.024**
Low expression		1	
High expression		1.5 (1.05-2.11)	

Abbreviations: HR: Hazard ratio, CI: Confidence interval, PSA: Prostate specific antigen, PSM: Positive surgical margin, NS: Not significant, No: Number, P: p-value).

Table 8: Results from the multivariate analysis for the expression of miR-20a-5p in TS (mean).

Characteristics	No	Biochemical failure	
		HR (95% CI)	P
Age			NS
< 65	333		
> 65	166		
Preop PSA			**0.008**
PSA < 10	291	1	
PSA > 10	208	0.67 (0.49-0.90)	
Missing			
Gleason grade group			**0.022**
1 (3+3)	168	1	
2 (3+4)	282	1.30 (0.28-5.89)	0.740
3 (4+3)	17	2.33 (0.52-10.5)	0.272
4 (4+4)	29	2.54 (0.52-12.5)	0.251
5 (>9)	3	2.88 (0.64-13.0)	0.170
Positive surgical margin PSM			**0.001**
No	367	1	
Yes	132	0.53 (0.39-0.76)	
Tumour size			NS
< 20 mm	235		
> 20 mm	264		
pT stage			**0.001**
pT2	357	0.98 (0.64-1.52)	0.949
pT3a	99	1.60 (0.84-3.03)	0.153
pT3b	43	0.59 (0.37-0.94)	**0.028**
miR-20a-5p in stroma (mean)			**0.026**
Low expression		1	
High expression		1.4 (1.04-1.92)	

Abbreviations: HR: Hazard ratio, CI: Confidence interval, PSA: Prostate specific antigen, PSM: Positive surgical margin, NS: Not significant, No: Number, P: p-value).

4 Discussion

With approximately 1.6 million new cases each year globally, PCa represents a massive challenge, and is the second most frequent cancer type occurring in men. In Norway, PCa is the most common form of cancer in men, and around 5.000 patients are diagnosed each year. In this study, consisting of 535 patients, we have examined the *in situ* tissue distribution of miR-17-5p and miR-20a-5p in PCa tissue and their potential functions as biomarkers, and assessed their prognostic value in PCa. We retrospectively evaluated the prognostic impact of marker expression in the clinical outcome Biochemical failure, Clinical failure, and Prostate cancer death by utilizing survival analyses. In addition, we correlated the miRNAs miR-17-5p and miR-20a-5p with the proliferation marker Ki-67.

Main findings

Interestingly, we found that high expression of both miR-17-5p and miR-20a-5p was associated with increased risk of having reduced time before BF. The expression of miR-17-5p was located in TE and for miR-20a-5p a high expression was seen in both TE and TS. The latter was confirmed by univariate and multivariate analysis.

Expression of Ki-67 is associated with proliferating cancer cells and poor prognosis and is furthermore broadly accepted as a reliable proliferation marker in multiple cancers [110, 127, 128]. Our results showed a powerful correlation between the expression of miR-17-5p and Ki-67. Moreover, our results showed a positive correlation between the expression of miR-20a-5p and Ki-67. A recent study by Emami and colleagues [129], inspected the expression of five miRNAs including miR-20a in Colorectal cancer and correlated the expression levels of the miRNAs with Ki-67, using Pearson correlation coefficient. Their results showed a significant positive correlation between miR-20a and Ki-67 ($r = 0.871$, $p < 0.001$) [129]. This is in line with our findings and supports our hypothesis of a possible correlation between miR-20a-5p and Ki-67 in PCa.

The oncomiRs in the miR-17-92 cluster represents attractive candidates as cancer biomarkers

miRNAs in the miR-17-92 cluster including miR-17-5p and miR-20a-5p, have in several studies demonstrated to act as oncogenes in PCa [94, 96, 97, 130]. miR-17 and miR-20a have been reported to negatively regulate the expression of E2F1 which promotes G_1 to S phase transition in mammalian cells, which consequentially shifts the balance from an apoptotic state into proliferation, thus indicating a possible anti-apoptotic role of these two miRNAs [86]. This anti-apoptotic role for the members of the miR-17-92 cluster have further been observed in other studies which have reported their roles in inducing apoptosis and promoting proliferation [131, 132]. Moreover, a previous study by Sylvestre and colleagues [133], implied oncogenic abilities of miR-20a when overexpressed, by acting on crucial cell cycle regulators and apoptosis [133]. Members of the miR-17-92 cluster have also been associated with PCa progression, where a study in 2013 by Yang *et al.* [134] confirmed that miR-17-5p and its passenger strand miR-17-3p targeted metallopeptidase inhibitor 3 (involved in degradation of the extracellular matrix) which lead to inducing prostate tumour growth and invasion [134].

The suggested role of miR-20a as a PCa biomarker are supported by Feng *et al*. [97] who presented a study which demonstrated upregulation of the miR-17-92 cluster in PCa tissue samples compared to BPH serving as control tissue, assessing a role as oncogenic contributors in PCa [97]. Interestingly, their study also showed that the miR-17-92 cluster could potentially be used as prognostic and diagnostic biomarkers for PCa [97]. Additionally, miR-20-5a was reported as a diagnostic biomarker for the identification of PCa in a recent study from 2017 by Daniel *et al*. [135] which presented a panel of seven miRNAs including miR-20a-5p, as proposed diagnostic biomarkers in PCa, however also emphasized the necessity of excessive validation and additional solid studies [135]. miR-20a is furthermore evaluated as a promising biomarker in several other cancers such as lung cancer, breast cancer, and gastric cancer [136-139]. Based on the above-mentioned studies highlighting the oncogenic characteristics of miR-17-5p and miR-20a-5p, it is convincible that these miRNAs are interesting candidates as biomarkers in cancer prognostics.

A strength in this thesis was the advantage of investigating TE, TS, and TE + TS separately which in some cases can be of interest to explore several various interplays between the targets of interest. Despite the ISH technique requiring relatively large workforce, it harbours great ability to assess marker expression in both TE, TS and down to cellular level. These abilities are attractive in PCa since this cancer type is known for its multifocal nature of tumour tissue.

Cut-off threshold

There is no defined cut-off threshold score of miR-17-5p or miR-20a-5p. In this study, the miRNA scores were dichotomized to separate as follows: low scores were defined as < mean/median, and high score as > mean/median, which is equivalent to a percentage staining of cancer cells of approximately 2.4%-2.5%. Staining ≥ 5 % was defined as strong staining. The chosen cut-off threshold might have a significant impact on the statistical analysis. All possible cut-offs were tested for each miRNA, and in each case, values that provided the most adequate statistical power was selected as the chosen cut-off.

Multicentre prostate cohort

A another strength in this thesis is the relatively large PCa patient cohort collected from three hospitals in central and northern Norway, which collectively accounts for 535 patients. The patient cohort is collected between the 10-year period 1995 to 2005, which falls into the area where the PSA test was introduced in Norway. This introduction lead to more active diagnosis of PCa, and detection of indolent disease [7]. Based on this, it is conceivable that our material is more comparable and homogeneous compared to material that would be collected before the introduction of PSA.

Furthermore, this retrospectively study provide some advantages considering the limited time period intended for a thesis as such. Unlike e.g. prospective studies, retrospective studies are more time efficient and with reduced expenses. It is appropriate for studying long latency diseases, since the events already have occurred, and awaiting disease progression is impossible. Although, retrospective studies have its limitations, where one

important limitation is the access to supplementary information like comorbidities and the individual life style of the patients. Also, collecting additional material of interest is not possible, like more tissue samples or blood samples. Another disadvantage is that retrospective studies are based on previously recorded information, which thus is affected to registry or memory bias when retrieving data. Another limitation that is important to note is the inconsistency, meaning that definitions of diseases may be modified, which is a natural occurring phenomenon as time passes, especially since technology development and continuous studies provide increased overall knowledge of a given disease.

Tissue fixation, processing and procedure

In this thesis FFPE tissue blocks of prostate tissue was used from the PCa patient multicentre cohort. FFPE blocks are greatly beneficial due to storage capabilities, considering the ability to be stored over many years and still perform stable immunostaining [140-142]. Furthermore, the need for fresh tissue is eliminated, and it preserves tissue morphology. Regarding tumour representation, it is most favourable to collect discrete samples that captures the tumour state at the site of biopsy. Also, multiple biopsy specimens should be collected to avoid missing tumour heterogeneity. Notably, preserving FFPE over several years may lead to some challenges. There is a risk of loss of tissue elasticity which may lead to technical challenges when obtaining cylindrical cores for TMA construction [143]. Since sampling sections from TMA technically is more challenging compared to whole tissue sections, some tissue loss should be taken into consideration. Herein, the cohort suffered from some cores scored as “missing”, which was expected beforehand.

TMA procedure is both time and cost effective, and a major benefit is the tissue utilization. The time and cost effectiveness can be explained by the clear benefit of staining a few TMA sections, compared to staining several more whole tissue sections, in addition minimizing the use of laboratory reagents [144]. TMAs are frequently used for a large variety of studies, including studies of tumour biology, assessing new diagnostic tools, and estimating the diagnostic accuracy of a biomarker of interest [145, 146]. TMA often represents around a thousand tumours, which corresponds to significant savings in scientific resources. In

addition, this also provides the advantage of reduced technical variability during the process of staining and interpretation. The close proximity of cores allows more consistent and rapid scoring of biomarkers [144].

In this thesis, an experienced pathologist identified representative prostate specimen areas for both normal and tumour epithelial and stromal cells, which is important to ascertain optimal tissue representativeness. As previously mentioned, PCa is known to be heterogenous, and is an example of a type of cancer that presents shifting grades of heterogeneity [147]. It is a cancer type that grows multifocal, thus high-risk areas are challenging to predict when choosing representative areas, hence the chosen tissue samples might not originate from the highest risk areas that represents the severity of the disease. Nevertheless, biomarker expression in TMAs have demonstrated good reproducibility compared to whole section [148].

When investigating biomarker expression in PCa, the tumour heterogeneity is taken into consideration when choosing the optimal number of cores representing each patient. When using a large PCa cohort (n = 535), three or four cores is optimally in such investigations, and also benefit from potential sampling errors that may occur. In this case, four cores in average were collected per patient, where two or more represented the dominant tumour. To limit potential background staining, which may happen when cutting TMA sections too thick, our TMA sections were cut 4 µm, subsequently attached to slides and sealed with paraffin.

ISH technique and methodology

Various techniques have been constructed with the intent to study the function, expression and structure of miRNAs. ISH is perhaps the technique demanding most workforce and time, in addition to a relatively decent skill requirement. ISH can be considered as a semiquantitative technique [149]. Still, valid advantages in detection and identification of miRNAs, and the ability to provide improved insight in diverse biological processes, makes ISH superior and a preferred choice over simpler techniques, such as Northern blot and quantitative Polymerase Chain Reaction (qPCR). The simpler techniques mentioned are

dependable, fast, and uncomplicated, which portrays their broad use in identifying miRNAs, and determining their absolute or relative expression level. Unfortunately, since these types of techniques relies on purified miRNAs [150-152], they fail to determine the specific cell types expressing the target miRNAs, for example in cases where expression levels are correlated with alterations in cell morphology, or where difference in expression levels are caused by a reduction or gain in a specific cell type population.

ISH provides the opportunity to investigate the cellular localization and the macroscopic distribution of DNA and RNA sequences in cell populations that are heterogenous. Thus, ISH is preferred in studies aiming to investigate miRNAs in tissues like tumour, like in this thesis, where ISH was chosen to investigate miRNA distribution in PCa tissue. Moreover, due to the short lengths of miRNAs, which are approximately 20 nucleotides, it decreases sequence specificity, and utilizing traditional RNA or DNA probes is furthermore challenging for detection due to risk of high background noise. LNA™ oligonucleotides have more or less eliminated this problem with their characteristic structure where the ribose ring is "locked" between the 2’ oxygen and the 4’ carbon by a methylene linkage [98]. Thus, LNA™ oligonucleotides provides more stability of the resulting duplexes when pairing with a complementary nucleotide strand, and also LNA™ oligonucleotides can still retain a high Tm despite being constructed shorter than the conventional RNA oligonucleotide, which is favourable when detecting highly similar or small targets [102].

There is no uniform methodology today for miR-17-5p or miR-20a-5p. Despite the access to automated equipment, fully standardized ISH methods is challenging, which may affect the reproducibility. Importantly, oligonucleotide probes behave differently in various tissues, and requires individual protocols to be made based on the characteristics of the probe, such as the length of the probe and the RNA Tm, which is listed by the manufacturer. In this thesis, miR-17-5p and miR-20a-5p did not cause major challenges, although thorough probe optimization was necessary in both cases. miR-17-5p showed good and strong staining after final optimization with a probe concentration of 20 nM, whereas miR-20a-5p showed only moderate staining with a notably high probe concentration of 50 nM. Target miRNA

representation is a depending factor when choosing the optimal probe concentration on the selected tissue. It must to be taken into consideration that miRNAs vary in abundance in different tissues and may be an explanation why miR-20a-5p did not show equally strong staining as miR-17-5p. Nevertheless, both miRNAs obtained satisfactory staining results in regards of scoring intensity and density in TE and TS.

During ISH, some pitfalls are important to be aware of, which in this thesis were evaluated beforehand, especially during probe optimization. Several factors may affect the final result of ISH, such as the condition of the tissue before, during fixation, and after fixation. Importantly, since RNA is highly sensitive to degradation, we always worked with RNase-free equipment and MilliQ purified water to avoid unnecessary contamination. Double-DIG labelled LNA™ probes are optimal in detecting miRNAs since they generate minimal background staining, hence being a favourable choice in this thesis [122]. Potential high or low background is also determined by the stringency washes. The stringency washes performed in our protocols was done with the same temperatures as used under the hybridization, unique for each probe, resulting in satisfactory staining without unnecessary background. Although the technique requires experience and is relatively time consuming, ISH is a reliable and thoroughly studied technique, which today are preferred in several different studies, including detection of miRNAs and molecular markers [118, 149, 153, 154].

To the degree of our knowledge, there are no similar multicentre studies of miR-17-5p and miR-20a-5p correlated to PCa with a relatively large PCa cohort (n = 535). There is still an ongoing discussion around the concern of overtreatment and overdiagnosis in PCa, which potentially may cause risk of adverse side effects. This ongoing controversy underlines the need for more personalized diagnosis and treatment of these patients, whereas miRNAs as biomarkers proposes as promising candidates.

5 Conclusion

Based on a large PCa cohort of 535 patients we investigated the prognostic role of miR-17-5p and miR-20a-5p in PCa tissue by *in situ* hybridization using univariate- and multivariate analyses. We found high expression of miR-17-5p and miR-20a-5p to be associated with increased risk of having reduced time before BF. The expression of miR-17-5p was located in TE and high miR-20a-5p expression was seen in both TE and TS. High miR-20a-5p expression was confirmed by both univariate and multivariate analysis. We found that high expression miR-20a-5p is a significant independent prognosticator for BF in TE + TS, and TE and TS separately. Furthermore, our results showed a positive correlation between the expression of the miRNAs miR-17-5p, miR-20a-5p and Ki-67.

The findings in this thesis suggests that miR-17-5p and miR-20a-5p may provide important information regarding prognosis in PCa, and also suggests a potential correlation between the miRNAs and Ki-67. The expression levels of the miRNAs and their correlation with the proliferation marker, makes them valuable as potential biomarkers in cancer detection and in predicting prognosis in patients suffering from PCa.

6 References

1. Denmeade SR, Isaacs JT, *A history of prostate cancer treatment.* Nat Rev Cancer, 2002. **2**(5): p. 389-96.
2. Hassanipour-Azgomi S, Mohammadian-Hafshejani A, Ghoncheh M, Towhidi F, Jamehshorani S, Salehiniya H, *Incidence and mortality of prostate cancer and their relationship with the Human Development Index worldwide.* Prostate Int, 2016. **4**(3): p. 118-24.
3. Ferlay J, Steliarova-Foucher E, Lortet-Tieulent J, Rosso S, Coebergh JW, Comber H, Forman D, Bray F, *Cancer incidence and mortality patterns in Europe: estimates for 40 countries in 2012.* Eur J Cancer, 2013. **49**(6): p. 1374-403.
4. Maia MC, Hansen AR, *A comprehensive review of immunotherapies in prostate cancer.* Crit Rev Oncol Hematol, 2017. **113**: p. 292-303.
5. Fitzmaurice C *et al*. *Global, Regional, and National Cancer Incidence, Mortality, Years of Life Lost, Years Lived With Disability, and Disability-Adjusted Life-years for 32 Cancer Groups, 1990 to 2015: A Systematic Analysis for the Global Burden of Disease Study.* JAMA Oncol, 2017. **3**(4): p. 524-548.
6. American Cancer Society, *Cancer Facts & Figures 2018*. 2018 [cited 20.02.2019]; [Available from: https://www.cancer.org/content/dam/cancer-org/research/cancer-facts-and-statistics/annual-cancer-facts-and-figures/2018/cancer-facts-and-figures-2018.pdf].
7. Kreftregisteret, *Årsrapport 2017 med resultater og forbedringstiltak fra Nasjonalt kvalitetsregister for prostatakreft*. 2018 [cited 20.02.2019]; [Available from: https://www.kreftregisteret.no/globalassets/publikasjoner-og-rapporter/arsrapporter/publisert-2018/arsrapport-2017-prostatakreft.pdf].
8. Lee CH, Akin-Olugbade O, Kirschenbaum A, *Overview of prostate anatomy, histology, and pathology.* Endocrinol Metab Clin North Am, 2011. **40**(3): p. 565-75, viii-ix.
9. Harvard University, H. *Prostate Basics* 2011 [cited 26.09.2018]; [Available from: https://www.harvardprostateknowledge.org/prostate-basics].
10. Aaron L, Franco OE, Hayward SW, *Review of Prostate Anatomy and Embryology and the Etiology of Benign Prostatic Hyperplasia.* Urol Clin North Am, 2016. **43**(3): p. 279-88.
11. Bhavsar A, Verma S, *Anatomic imaging of the prostate.* Biomed Res Int, 2014. **2014**: p. 728539.
12. Oh WK, Hurwitz M, D'Amico AV, Richie JP, Kantoff, PW, *Biology of Prostate Cancer,* ed. Kufe DW, Pollock RE, Weichselbaum RR. Holland-Frei Cancer Medicine. 6th edition. Hamilton (ON): BC Decker; 2003; [Available from: https://www.ncbi.nlm.nih.gov/books/NBK13217/].
13. Helsenorge, *Prostatakreft* 2019 [cited 18.03.2019]; [Available from: https://helsenorge.no/sykdom/kreft/prostatakreft].
14. Prostatakreftforeningen, *Symptomer* 2019 [cited 18.03.2019]; [Available from: https://www.prostatakreft.no/symptomer/].
15. De Angelis G, Rittenhouse HG, Mikolajczyk SD, Blair Shamel L, Semjonow A, *Twenty Years of PSA: From Prostate Antigen to Tumor Marker.* Rev Urol, 2007. **9**(3): p. 113-23.

16. Adhyam M, Gupta AK, *A Review on the Clinical Utility of PSA in Cancer Prostate.* Indian J Surg Oncol, 2012. **3**(2): p. 120-9.
17. Oesterling JE, Jacobsen SJ, Chute CG, Guess HA, Girman CJ, Panser LA, Lieber MM, *Serum prostate-specific antigen in a community-based population of healthy men. Establishment of age-specific reference ranges.* Jama, 1993. **270**(7): p. 860-4.
18. Atan A, Guzel O, *How should prostate specific antigen be interpreted?* Turk J Urol, 2013. **39**(3): p. 188-93.
19. Balk SP, Ko YJ, Bubley GJ, *Biology of prostate-specific antigen.* J Clin Oncol, 2003. **21**(2): p. 383-91.
20. Lilja H, *Structure, function, and regulation of the enzyme activity of prostate-specific antigen.* World J Urol, 1993. **11**(4): p. 188-91.
21. Scher HI, *Prostate carcinoma: defining therapeutic objectives and improving overall outcomes.* Cancer, 2003. **97**(3 Suppl): p. 758-71.
22. Aggarwal RR, Feng FY, Small EJ, *Emerging Categories of Disease in Advanced Prostate Cancer and Their Therapeutic Implications.* Oncology (Williston Park), 2017. **31**(6): p. 467-74.
23. Epstein JI, Amin MB, Reuter VE, Humphrey PA, *Contemporary Gleason Grading of Prostatic Carcinoma: An Update With Discussion on Practical Issues to Implement the 2014 International Society of Urological Pathology (ISUP) Consensus Conference on Gleason Grading of Prostatic Carcinoma.* Am J Surg Pathol, 2017. **41**(4): p. e1-e7.
24. Prostate Conditions Education Council, *Gleason Score Prostate Cancer Grading & Prognostic Scoring*. 2019 [cited 11.03.2019]; [Available from: https://www.prostateconditions.org/about-prostate-conditions/prostate-cancer/newly-diagnosed/gleason-score].
25. Chen N, Zhou Q, *The evolving Gleason grading system.* Chin J Cancer Res, 2016. **28**(1): p. 58-64.
26. Gordetsky J, Epstein J, *Grading of prostatic adenocarcinoma: current state and prognostic implications.* Diagn Pathol, 2016. **11**: p. 25.
27. Epstein JI, Egevad L, Amin MB, Delahunt B, Srigley JR, Humphrey PA, *The 2014 International Society of Urological Pathology (ISUP) Consensus Conference on Gleason Grading of Prostatic Carcinoma: Definition of Grading Patterns and Proposal for a New Grading System.* Am J Surg Pathol, 2016. **40**(2): p. 244-52.
28. Epstein JI *et al*. *A Contemporary Prostate Cancer Grading System: A Validated Alternative to the Gleason Score.* Eur Urol, 2016. **69**(3): p. 428-35.
29. Mottet N *et al*. *EAU - ESTRO - ESUR - SIOG Guidelines on Prostate Cancer*. European Association of Urology. 2017 [cited 13.04.2019]; [Avaliable from: https://uroweb.org/wp-content/uploads/09-Prostate-Cancer_2017_web.pdf].
30. Solberg A *et al*. *Nasjonalt handlingsprogram med retningslinjer for diagnostikk, behandling og oppfølging av prostatakreft*. 7th edition. Helsedirektoratet; 2015 [cited 22.10.2018]; [Avaliable from: https://www.helsebiblioteket.no/retningslinjer/prostatakreft/innhold].
31. Jayadevappa R *et al*. *Comparative effectiveness of prostate cancer treatments for patient-centered outcomes: A systematic review and meta-analysis (PRISMA Compliant).* Medicine (Baltimore), 2017. **96**(18): p. e6790.

32. Moschini M, Carroll PR, Eggener SE, Epstein JI, Graefen M, Montironi R, Parker C, *Low-risk Prostate Cancer: Identification, Management, and Outcomes.* Eur Urol, 2017. **72**(2): p. 238-249.
33. Chen FZ, Zhao XK, *Prostate cancer: current treatment and prevention strategies.* Iran Red Crescent Med J, 2013. **15**(4): p. 279-84.
34. Lee JY *et al*. *A competing risk analysis of cancer-specific mortality of initial treatment with radical prostatectomy versus radiation therapy in clinically localized high-risk prostate cancer.* Ann Surg Oncol, 2014. **21**(12): p. 4026-33.
35. Komura K, Sweeney CJ, Inamoto T, Ibuki N, Azuma H, Kantoff PW, *Current treatment strategies for advanced prostate cancer.* Int J Urol, 2018. **25**(3): p. 220-231.
36. Chang AJ, Autio KA, Roach M, Scher HI, *High-risk prostate cancer-classification and therapy.* Nat Rev Clin Oncol, 2014. **11**(6): p. 308-23.
37. Kim SJ, Kim SI, *Current treatment strategies for castration-resistant prostate cancer.* Korean J Urol, 2011. **52**(3): p. 157-65.
38. McKeage K, *Docetaxel: a review of its use for the first-line treatment of advanced castration-resistant prostate cancer.* Drugs, 2012. **72**(11): p. 1559-77.
39. Gandhi J, Afridi A, Vatsia S, Joshi G, Joshi, G, Kaplan SA, Smith NL, Khan SA, *The molecular biology of prostate cancer: current understanding and clinical implications.* Prostate Cancer Prostatic Dis, 2018. **21**(1): p. 22-36.
40. Benafif S, Eeles R, *Genetic predisposition to prostate cancer.* Br Med Bull, 2016. **120**(1): p. 75-89.
41. Shan M *et al. Molecular analyses of prostate tumors for diagnosis of malignancy on fine-needle aspiration biopsies.* Oncotarget, 2017. **8**(62): p. 104761-104771.
42. Patel R, Khalifa AO, Isali I, Shukla S, *Prostate cancer susceptibility and growth linked to Y chromosome genes.* Front Biosci (Elite Ed), 2018. **10**: p. 423-436.
43. Martinez-Gonzalez LJ, Pascual Geler M, Robles Fernandez I, Cozar JM, Lorente JA, Alvarez Cubero MJ, *Improving the genetic signature of prostate cancer, the somatic mutations.* Urol Oncol, 2018. **36**(6): p. 312.e17-312.e23.
44. Wu YM *et al*. *Inactivation of CDK12 Delineates a Distinct Immunogenic Class of Advanced Prostate Cancer.* Cell, 2018. **173**(7): p. 1770-1782.e14.
45. Viswanathan SR *et al. Structural Alterations Driving Castration-Resistant Prostate Cancer Revealed by Linked-Read Genome Sequencing.* Cell, 2018. **174**(2): p. 433-447.e19.
46. Yoshimoto M, Ludkovski O, DeGrace D, Williams JL, Evans A, Sircar K, Bismar TA, Nuin P, Squire JA, *PTEN genomic deletions that characterize aggressive prostate cancer originate close to segmental duplications.* Genes Chromosomes Cancer, 2012. **51**(2): p. 149-60.
47. Lou W *et al*. *MicroRNAs in cancer metastasis and angiogenesis.* Oncotarget, 2017. **8**(70): p. 115787-115802.
48. Lin Y, Chen F, Shen L, Tang X, Du C, Sun Z, Ding H, Chen J, Shen B, *Biomarker microRNAs for prostate cancer metastasis: screened with a network vulnerability analysis model.* J Transl Med, 2018. **16**(1): p. 134.
49. Aghdam SG, Ebrazeh M, Hemmatzadeh M, Seyfizadeh N, Shabgah AG, Azizi G, Ebrahimi N, Babaie F, Mohammadi H, *The role of microRNAs in prostate cancer migration, invasion, and metastasis.* J Cell Physiol, 2019. **234**(7): p. 9927-9942.

50. Broughton JP, Lovci MT, Huang JL, Yeo GW, Pasquinelli AE, *Pairing beyond the Seed Supports MicroRNA Targeting Specificity.* Mol Cell, 2016. **64**(2): p. 320-333.
51. Juzenas S *et al*. *A comprehensive, cell specific microRNA catalogue of human peripheral blood.* Nucleic Acids Res, 2017. **45**(16): p. 9290-9301.
52. Vanacore D *et al*. *Micrornas in prostate cancer: an overview.* Oncotarget, 2017. **8**(30): p. 50240-50251.
53. Tan W, Liu B, Qu S, Liang G, Luo W, Gong C, *MicroRNAs and cancer: Key paradigms in molecular therapy.* Oncol Lett, 2018. **15**(3): p. 2735-2742.
54. Hosseinahli N, Aghapour M, Duijf PHG, Baradaran B, *Treating cancer with microRNA replacement therapy: A literature review.* J Cell Physiol, 2018. **233**(8): p. 5574-5588.
55. Rupaimoole R, Slack FJ, *MicroRNA therapeutics: towards a new era for the management of cancer and other diseases.* Nat Rev Drug Discov, 2017. **16**(3): p. 203-222.
56. Hanahan D, Weinberg RA, *The hallmarks of cancer.* Cell, 2000. **100**(1): p. 57-70.
57. Silber J, James CD, Hodgson JG, *microRNAs in gliomas: small regulators of a big problem.* Neuromolecular Med, 2009. **11**(3): p. 208-22.
58. Fang L *et al*. *MicroRNA miR-93 promotes tumor growth and angiogenesis by targeting integrin-beta8.* Oncogene, 2011. **30**(7): p. 806-21.
59. Onishi M, Ichikawa T, Kurozumi K, Date I, *Angiogenesis and invasion in glioma.* Brain Tumor Pathol, 2011. **28**(1): p. 13-24.
60. Wang S, Olson EN, *AngiomiRs--key regulators of angiogenesis.* Curr Opin Genet Dev, 2009. **19**(3): p. 205-11.
61. Landskroner-Eiger S, Moneke I, Sessa WC, *miRNAs as modulators of angiogenesis.* Cold Spring Harb Perspect Med, 2013. **3**(2): p. a006643.
62. Wurdinger T, Tannous BA, Saydam O, Skog J, Grau S, Soutschek J, Weissleder R, Breakefield XO, Krichevsky AM, *miR-296 regulates growth factor receptor overexpression in angiogenic endothelial cells.* Cancer Cell, 2008. **14**(5): p. 382-93.
63. Rao Z, He Z, He Y, Guo Z, Kong D, Liu J, *MicroRNA5123p is upregulated, and promotes proliferation and cell cycle progression, in prostate cancer cells.* Mol Med Rep, 2018. **17**(1): p. 586-593.
64. Andersen S, Richardsen E, Moi L, Donnem T, Nordby Y, Ness N, Holman ME, Bremnes RM, Busund LT, *Fibroblast miR-210 overexpression is independently associated with clinical failure in Prostate Cancer - a multicenter (in situ hybridization) study.* Sci Rep, 2016. **6**: p. 36573.
65. Li JZ, Li J, Wang HQ, Li X, Wen B, Wang YJ, *MiR-141-3p promotes prostate cancer cell proliferation through inhibiting kruppel-like factor-9 expression.* Biochem Biophys Res Commun, 2017. **482**(4): p. 1381-1386.
66. Yang ZG, Ma XD, He ZH, Guo YX, *miR-483-5p promotes prostate cancer cell proliferation and invasion by targeting RBM5.* Int Braz J Urol, 2017. **43**(6): p. 1060-1067.
67. Shao N, Ma G, Zhang J, Zhu W, *miR-221-5p enhances cell proliferation and metastasis through post-transcriptional regulation of SOCS1 in human prostate cancer.* BMC Urol, 2018. **18**(1): p. 14.

68. Gui B, Hsieh CL, Kantoff PW, Kibel AS, Jia L, *Androgen receptor-mediated downregulation of microRNA-221 and -222 in castration-resistant prostate cancer.* PLoS One, 2017. **12**(9): p. e0184166.
69. Huang W, *MicroRNAs: Biomarkers, Diagnostics, and Therapeutics.* Methods Mol Biol, 2017. **1617**: p. 57-67.
70. Detassis S, Grasso M, Del Vescovo V, Denti MA, *microRNAs Make the Call in Cancer Personalized Medicine.* Front Cell Dev Biol, 2017. **5**: p. 86.
71. Richardsen E, *et al*. *MicroRNA 141 is associated to outcome and aggressive tumor characteristics in prostate cancer.* Sci Rep, 2019. **9**(1): p. 386.
72. Nordby Y, Richardsen E, Ness N, Donnem T, Patel HRH, Busund LT, Bremnes RM, Andersen S, *High miR-205 expression in normal epithelium is associated with biochemical failure - an argument for epithelial crosstalk in prostate cancer?* Sci Rep, 2017. **7**(1): p. 16308.
73. Melbo-Jorgensen C *et al*. *Stromal expression of MiR-21 predicts biochemical failure in prostate cancer patients with Gleason score 6.* PLoS One, 2014. **9**(11): p. e113039.
74. Eilertsen M *et al*. *Positive prognostic impact of miR-210 in non-small cell lung cancer.* Lung Cancer, 2014. **83**(2): p. 272-8.
75. Donnem T *et al*. *Prognostic impact of MiR-155 in non-small cell lung cancer evaluated by in situ hybridization.* J Transl Med, 2011. **9**: p. 6.
76. Skjefstad K *et al*. *A gender specific improved survival related to stromal miR-143 and miR-145 expression in non-small cell lung cancer.* Sci Rep, 2018. **8**(1): p. 8549.
77. Bhaskaran M, Mohan M, *MicroRNAs: history, biogenesis, and their evolving role in animal development and disease.* Vet Pathol, 2014. **51**(4): p. 759-74.
78. Thermo Fisher, *miRNA Biogenesis*. 2018 [cited 27.09.2018]; [Available from: https://www.thermofisher.com/no/en/home/life-science/epigenetics-noncoding-rna-research/epigenetics-learning-center/mirna/mirna-biogenesis.html].
79. Macfarlane LA, Murphy PR, *MicroRNA: Biogenesis, Function and Role in Cancer.* Curr Genomics, 2010. **11**(7): p. 537-61.
80. Ha M, Kim VN, *Regulation of microRNA biogenesis.* Nat Rev Mol Cell Biol, 2014. **15**(8): p. 509-24.
81. Winter J, Jung S, Keller S, Gregory RI, Diederichs S, *Many roads to maturity: microRNA biogenesis pathways and their regulation.* Nat Cell Biol, 2009. **11**(3): p. 228-34.
82. Guo J, Mei Y, Li K, Huang X, Yang H, *Downregulation of miR-17-92a cluster promotes autophagy induction in response to celastrol treatment in prostate cancer cells.* Biochem Biophys Res Commun, 2016. **478**(2): p. 804-10.
83. Luu HN *et al*. *miRNAs associated with prostate cancer risk and progression.* BMC Urol, 2017. **17**(1): p. 18.
84. Mogilyansky E, Rigoutsos I, *The miR-17/92 cluster: a comprehensive update on its genomics, genetics, functions and increasingly important and numerous roles in health and disease.* Cell Death Differ, 2013. **20**(12): p. 1603-14.
85. Concepcion CP, Bonetti C, Ventura A, *The microRNA-17-92 family of microRNA clusters in development and disease.* Cancer J, 2012. **18**(3): p. 262-7.
86. Gruszka R, Zakrzewska M, *The Oncogenic Relevance of miR-17-92 Cluster and Its Paralogous miR-106b-25 and miR-106a-363 Clusters in Brain Tumors.* Int J Mol Sci, 2018. **19**(3).

87. Tanzer A, Stadler PF, *Molecular evolution of a microRNA cluster.* J Mol Biol, 2004. **339**(2): p. 327-35.
88. Mendell JT, *miRiad roles for the miR-17-92 cluster in development and disease.* Cell, 2008. **133**(2): p. 217-22.
89. Brancati G, Grosshans H, *An interplay of miRNA abundance and target site architecture determines miRNA activity and specificity.* Nucleic Acids Res, 2018. **46**(7): p. 3259-3269.
90. Bartel DP, *MicroRNAs: target recognition and regulatory functions.* Cell, 2009. **136**(2): p. 215-33.
91. Grimson A, Farh KK, Johnston WK, Garrett-Engele P, Lim LP, Bartel DP, *MicroRNA targeting specificity in mammals: determinants beyond seed pairing.* Mol Cell, 2007. **27**(1): p. 91-105.
92. Lewis BP, Shih IH, Jones-Rhoades MW, Bartel DP, Burge CB, *Prediction of mammalian microRNA targets.* Cell, 2003. **115**(7): p. 787-98.
93. Zhou P, Ma L, Zhou J, Jiang M, Rao E, Zhao Y, Guo F, *miR-17-92 plays an oncogenic role and conveys chemo-resistance to cisplatin in human prostate cancer cells.* Int J Oncol, 2016. **48**(4): p. 1737-48.
94. Pesta M *et al*. *Importance of miR-20a expression in prostate cancer tissue.* Anticancer Res, 2010. **30**(9): p. 3579-83.
95. Qiang XF *et al*. *miR-20a promotes prostate cancer invasion and migration through targeting ABL2.* J Cell Biochem, 2014. **115**(7): p. 1269-76.
96. Olive V, Jiang I, He L, *mir-17-92, a cluster of miRNAs in the midst of the cancer network.* Int J Biochem Cell Biol, 2010. **42**(8): p. 1348-54.
97. Feng S, Qian X, Li H, Zhang X, *Combinations of elevated tissue miRNA-17-92 cluster expression and serum prostate-specific antigen as potential diagnostic biomarkers for prostate cancer.* Oncol Lett, 2017. **14**(6): p. 6943-6949.
98. Microsynth, *Locked Nucleic Acid (LNA)*. Increased Thermal Stability and Hybridization Specificity Improved Signal-to-Noise Ratio in qPCR Assays Enhanced Single Nucleotide Discrimination; [year unknown] [cited 26.09.2018]; [Available from: https://www.microsynth.ch/files/Inhalte/PDFs/Oligosynthesis/Flyer_Oligo_LNA.pdf].
99. Kubota K, Ohashi A, Imachi H, Harada H, *Improved in situ hybridization efficiency with locked-nucleic-acid-incorporated DNA probes.* Appl Environ Microbiol, 2006. **72**(8): p. 5311-7.
100. Exiqon, *Locked Nucleic Acid (LNA™) Technology*. 2017 [cited 29.01.2017]; [Available from: http://www.exiqon.com/lna-technology].
101. Walter BA, Valera VA, Pinto PA, Merino MJ, *Comprehensive microRNA Profiling of Prostate Cancer.* J Cancer, 2013. **4**(5): p. 350-7.
102. Exiqon, *Locked Nucleic Acid (LNA™), Custom Oligonucleotides for RNA and DNA Research.* 2009 [cited 26.09.2018]; [Available from: http://www.exiqon.com/ls/Documents/Scientific/LNA_folder.pdf].
103. Inwald EC, Klinkhammer-Schalke M, Hofstadter F, Zeman F, Koller M, Gerstenhauer M, Ortmann O, *Ki-67 is a prognostic parameter in breast cancer patients: results of a large population-based cohort of a cancer registry.* Breast Cancer Res Treat, 2013. **139**(2): p. 539-52.

104. Li S *et al*. *Extranodal NK/T-cell lymphoma, nasal type: a report of 73 cases at MD Anderson Cancer Center.* Am J Surg Pathol, 2013. **37**(1): p. 14-23.
105. Johannessen AL, Torp SH, *The clinical value of Ki-67/MIB-1 labeling index in human astrocytomas.* Pathol Oncol Res, 2006. **12**(3): p. 143-7.
106. Kankuri M, Soderstrom KO, Pelliniemi TT, Vahlberg T, Pyrhonen S, Salminen E, *The association of immunoreactive p53 and Ki-67 with T-stage, grade, occurrence of metastases and survival in renal cell carcinoma.* Anticancer Res, 2006. **26**(5b): p. 3825-33.
107. Munstedt K, von Georgi R, Franke FE, *Correlation between MIB1-determined tumor growth fraction and incidence of tumor recurrence in early ovarian carcinomas.* Cancer Invest, 2004. **22**(2): p. 185-94.
108. Scholzen T, Endl E, Wohlenberg C, van der Sar S, Cowell IG, Gerdes J, Singh PB, *The Ki-67 protein interacts with members of the heterochromatin protein 1 (HP1) family: a potential role in the regulation of higher-order chromatin structure.* J Pathol, 2002. **196**(2): p. 135-44.
109. Gerdes J, Lemke H, Baisch H, Wacker HH, Schwab U, Stein H, *Cell cycle analysis of a cell proliferation-associated human nuclear antigen defined by the monoclonal antibody Ki-67.* J Immunol, 1984. **133**(4): p. 1710-5.
110. Li LT, Jiang G, Chen Q, Zheng JN, *Ki67 is a promising molecular target in the diagnosis of cancer (review).* Mol Med Rep, 2015. **11**(3): p. 1566-72.
111. Fisher G, Yang ZH, Kudahetti S, Moller H, Scardino P, Cuzick J, Berney DM, *Prognostic value of Ki-67 for prostate cancer death in a conservatively managed cohort.* Br J Cancer, 2013. **108**(2): p. 271-7.
112. Rubio J, Ramos D, Lopez-Guerrero JA, Iborra I, Collado A, Solsona E, Almenar S, Llombart-Bosch A, *Immunohistochemical expression of Ki-67 antigen, cox-2 and Bax/Bcl-2 in prostate cancer; prognostic value in biopsies and radical prostatectomy specimens.* Eur Urol, 2005. **48**(5): p. 745-51.
113. Tolonen TT, Tammela TL, Kujala PM, Tuominen VJ, Isola JJ, Visakorpi T, *Histopathological variables and biomarkers enhancer of zeste homologue 2, Ki-67 and minichromosome maintenance protein 7 as prognosticators in primarily endocrine-treated prostate cancer.* BJU Int, 2011. **108**(9): p. 1430-8.
114. Vis AN, van Rhijn BW, Noordzij MA, Schroder FH, van der Kwast TH, *Value of tissue markers p27(kip1), MIB-1, and CD44s for the pre-operative prediction of tumour features in screen-detected prostate cancer.* J Pathol, 2002. **197**(2): p. 148-54.
115. Wolters T, Vissers KJ, Bangma CH, Schroder FH, van Leenders GJ, *The value of EZH2, p27(kip1), BMI-1 and MIB-1 on biopsy specimens with low-risk prostate cancer in selecting men with significant prostate cancer at prostatectomy.* BJU Int, 2010. **106**(2): p. 280-6.
116. Zellweger T *et al*. *Tumour growth fraction measured by immunohistochemical staining of Ki67 is an independent prognostic factor in preoperative prostate biopsies with small-volume or low-grade prostate cancer.* Int J Cancer, 2009. **124**(9): p. 2116-23.
117. Tollefson MK, Karnes RJ, Kwon ED, Lohse CM, Rangel LJ, Mynderse LA, Cheville JC,

Sebo TJ, *Prostate cancer Ki-67 (MIB-1) expression, perineural invasion, and gleason score as biopsy-based predictors of prostate cancer mortality: the Mayo model.* Mayo Clin Proc, 2014. **89**(3): p. 308-18.
118. Jensen E, *Technical review: In situ hybridization.* Anat Rec (Hoboken), 2014. **297**(8): p. 1349-53.
119. Zhang D, Xie L, Jin Y, *In situ Detection of MicroRNAs: The Art of MicroRNA Research in Human Diseases.* J Cytol Histol, 2015. **Suppl 3**(1).
120. Wilkinson DG, *In Situ Hybridization: A Practical Approach*. The Practical Approach Series, ed. B.D. Hames. 1999, United States, Oxford University Press Inc. New York: Oxford University Press.
121. Wolf RWC, Farfsing A, Tiantom J, Heller A, Bergauer T, Day W, Rueger B. *A Method for High Quality Digoxigenin-Labeled RNA Probes for In Situ Hybridization*. 2012 [cited 08.03.2019]; [Available from: https://www.sigmaaldrich.com/content/dam/sigma-aldrich/docs/Roche/General_Information/1/dig-application-note-iris.pdf].
122. QIAGEN, *Detection of miRNA by FFPE in situ hybridization (ISH) using double-labeled, LNAenhanced probes*. miRCURY® LNA® miRNA Detection Probes Handbook 2017; [Available from: https://www.qiagen.com/us/resources/resourcedetail?id=6cc49077-28a8-4a7b-8622-a739b7ed2c67&lang=en].
123. QIAGEN, *Oligo Dilution Calculator*. 2019 [cited 05.05.2019]; Available from: https://www.qiagen.com/us/resources/technologies/lna/custom-lna-design-and-applications/lna-design-tools-calculators/lna-dilution-calculator/.
124. Fisher RA, *Statistical methods for research workers*. 12th ed. Biological monographs and manuals, no. 5. 1954: Edinburgh, Oliver and Boyd.
125. Koo TK, Li MY, *A Guideline of Selecting and Reporting Intraclass Correlation Coefficients for Reliability Research.* J Chiropr Med, 2016. **15**(2): p. 155-63.
126. Richardsen E *et al*. *Evaluation of the proliferation marker Ki-67 in a large prostatectomy cohort.* PLoS One, 2017. **12**(11): p. e0186852.
127. Sun X, Kaufman PD, *Ki-67: more than a proliferation marker.* Chromosoma, 2018. **127**(2): p. 175-186.
128. Warth A *et al*. *Tumour cell proliferation (Ki-67) in non-small cell lung cancer: a critical reappraisal of its prognostic role.* Br J Cancer, 2014. **111**(6): p. 1222-9.
129. Emami SS, Akbari A, Zare AA, Agah S, Masoodi M, Talebi A, Minaeian S, Fattahi A, Moghadamnia F, *MicroRNA Expression Levels and Histopathological Features of Colorectal Cancer.* J Gastrointest Cancer, 2018.
130. Ottman R, Levy J, Grizzle WE, Chakrabarti R, *The other face of miR-17-92a cluster, exhibiting tumor suppressor effects in prostate cancer.* Oncotarget, 2016. **7**(45): p. 73739-73753.
131. Ranji N, Sadeghizadeh M, Shokrgozar MA, Bakhshandeh B, Karimipour M, Amanzadeh A, Azadmanesh K, *MiR-17-92 cluster: an apoptosis inducer or proliferation enhancer.* Mol Cell Biochem, 2013. **380**(1-2): p. 229-38.
132. Zhang W *et al*. *MicroRNA-17-92 cluster promotes the proliferation and the chemokine production of keratinocytes: implication for the pathogenesis of psoriasis.* Cell Death Dis, 2018. **9**(5): p. 567.

133. Sylvestre Y, De Guire V, Querido E, Mukhopadhyay UK, Bourdeau V, Major F, Ferbeyre G, Chartrand P, *An E2F/miR-20a autoregulatory feedback loop.* J Biol Chem, 2007. **282**(4): p. 2135-43.
134. Yang X, Du WW, Li H, Liu F, Khorshidi A, Rutnam ZJ, Yang BB, *Both mature miR-17-5p and passenger strand miR-17-3p target TIMP3 and induce prostate tumor growth and invasion.* Nucleic Acids Res, 2013. **41**(21): p. 9688-704.
135. Daniel R, Wu Q, Williams V, Clark G, Guruli G, Zehner Z, *A Panel of MicroRNAs as Diagnostic Biomarkers for the Identification of Prostate Cancer.* Int J Mol Sci, 2017. **18**(6).
136. Huang D, Peng Y, Ma K, Deng X, Tang L, Jing D, Shao Z, *MiR-20a, a novel promising biomarker to predict prognosis in human cancer: a meta-analysis.* BMC Cancer, 2018. **18**(1): p. 1189.
137. Zhang H, Mao F, Shen T, Luo Q, Ding Z, Qian L, Huang J, *Plasma miR-145, miR-20a, miR-21 and miR-223 as novel biomarkers for screening early-stage non-small cell lung cancer.* Oncol Lett, 2017. **13**(2): p. 669-676.
138. Luengo-Gil G, Gonzalez-Billalabeitia E, Perez-Henarejos SA, Navarro Manzano E, Chaves-Benito A, Garcia-Martinez E, Garcia-Garre E, Vicente V, Ayala de la Pena F, *Angiogenic role of miR-20a in breast cancer.* PLoS One, 2018. **13**(4): p. e0194638.
139. Yang R, Fu Y, Zeng Y, Xiang M, Yin Y, Li L, Xu H, Zhong J, Zeng X, *Serum miR-20a is a promising biomarker for gastric cancer.* Biomed Rep, 2017. **6**(4): p. 429-434.
140. Litlekalsoy J, Vatne V, Hostmark JG, Laerum OD, *Immunohistochemical markers in urinary bladder carcinomas from paraffin-embedded archival tissue after storage for 5-70 years.* BJU Int, 2007. **99**(5): p. 1013-9.
141. Grillo F, Bruzzone M, Pigozzi S, Prosapio S, Migliora P, Fiocca R, Mastracci L, *Immunohistochemistry on old archival paraffin blocks: is there an expiry date?* J Clin Pathol, 2017. **70**(11): p. 988-993.
142. Kokkat TJ, Patel MS, McGarvey D, LiVolsi VA, Baloch ZW, *Archived formalin-fixed paraffin-embedded (FFPE) blocks: A valuable underexploited resource for extraction of DNA, RNA, and protein.* Biopreserv Biobank, 2013. **11**(2): p. 101-6.
143. Fowler CB, Man YG, Zhang S, O'Leary TJ, Mason JT, Cunningham RE, *Tissue microarrays: construction and uses.* Methods Mol Biol, 2011. **724**: p. 23-35.
144. Voduc D, Kenney C, Nielsen TO, *Tissue microarrays in clinical oncology.* Semin Radiat Oncol, 2008. **18**(2): p. 89-97.
145. Mhawech-Fauceglia P, Herrmann FR, Bshara W, Odunsi K, Terracciano L, Sauter G, Cheney RT, Groth J, Penetrante R, *Friend leukaemia integration-1 expression in malignant and benign tumours: a multiple tumour tissue microarray analysis using polyclonal antibody.* J Clin Pathol, 2007. **60**(6): p. 694-700.
146. Kambham N, Kong C, Longacre TA, Natkunam Y, *Utility of syndecan-1 (CD138) expression in the diagnosis of undifferentiated malignant neoplasms: a tissue microarray study of 1,754 cases.* Appl Immunohistochem Mol Morphol, 2005. **13**(4): p. 304-10.
147. Tolkach Y, Kristiansen G, *The Heterogeneity of Prostate Cancer: A Practical Approach.* Pathobiology, 2018. **85**(1-2): p. 108-116.

148. Leversha MA, Fielding P, Watson S, Gosney JR, Field JK, *Expression of p53, pRB, and p16 in lung tumours: a validation study on tissue microarrays.* J Pathol, 2003. **200**(5): p. 610-9.
149. Gould BR, Damgaard T, Nielsen BS, *Chromogenic In Situ Hybridization Methods for microRNA Biomarker Monitoring of Drug Safety and Efficacy.* Methods Mol Biol, 2017. **1641**: p. 399-412.
150. Binderup HG, Madsen JS, Heegaard NHH, Houlind K, Andersen RF, Brasen CL, *Quantification of microRNA levels in plasma - Impact of preanalytical and analytical conditions.* PLoS One, 2018. **13**(7): p. e0201069.
151. Channavajjhala SK, Rossato M, Morandini F, Castagna A, Pizzolo F, Bazzoni F, Olivieri O, *Optimizing the purification and analysis of miRNAs from urinary exosomes.* Clin Chem Lab Med, 2014. **52**(3): p. 345-54.
152. McClure LV, Lin YT, Sullivan CS, *Detection of viral microRNAs by Northern blot analysis.* Methods Mol Biol, 2011. **721**: p. 153-71.
153. McGlinn E, Holzman MA, Mansfield JH, *Detection of Gene and Protein Expression in Mouse Embryos and Tissue Sections.* Methods Mol Biol, 2019. **1920**: p. 183-218.
154. Nielsen BS, Holmstrom K, *Combined microRNA in situ hybridization and immunohistochemical detection of protein markers.* Methods Mol Biol, 2013. **986**: p. 353-65.

7 Appendix

Table 9: Table presenting values from the Oligo Dilution Calculator, delivered by Qiagen. Stock concentration, stock volume and desired target concentration were entered for the positive and negative controls U6 and Scramble miR, to calculate water/buffer ratio (1:1), and total volume.

Probe	Stock concentration	Volume	Target concentration	Water/Buffer	Total volume
(miR-17-5p) U6	25 nM	6 µL	1.5 nM	94 µL	100 µL
(miR-17-5p) Scramble miR	100 nM	15 µL	10 nM	135 µL	150 µL
(miR-20a-5p) U6	25 nM	9 µL	1.5 nM	141 µL	150 µL
(miR-20a-5p) Scramble miR	100 nM	15 µL	10 nM	135 µL	150 µL

Table 10: Overview of the ChromoMap™ Blue Kit, anti-DIG, and Antibody block used in the *in situ* hybridization.

Kit name	Catalog number	Components	Manufacturer
ChromoMap™ Blue Kit	760-161	Activator CM (For increasing signal intensity) NBT CM (Hue enhancer) BCIP CM (Substrate for Alkaline Phosphatase)	Ventana Medical Systems, INC. /ROCHE
DISCOVERY anti-DIG AP Multimer (RUO)	760-4825	One 5 mL dispenser of DISCOVERY anti-DIG AP Multimer (RUO) contains reagent for 50 tests	Ventana Medical Systems, INC. /ROCHE
DISCOVERY Antibody Block	760-4204	Blocking reagent for IHC and ISH, High ionic strength protein reagent	Ventana Medical Systems, INC. /ROCHE

Abbreviations: NBT: 4-nitro-blue tetrazolium, BCIP: 5-bromo-4-chloro-3' indolylphosphate, AP: Alkaline Phosphatase, DIG: Digoxigenin, RUO: Research Use Only.